Structure-based Virtual Screening and Molecular Dynamics Simulations For Detecting Novel Candidates as FGFR1 Inhibitors

Güneş Çoban[1*]

[1]Department of Pharmaceutical Chemistry, Faculty of Pharmacy, Ege University, 35040 Bornova, Izmir, Turkey

***Corresponding author**

Table of contents

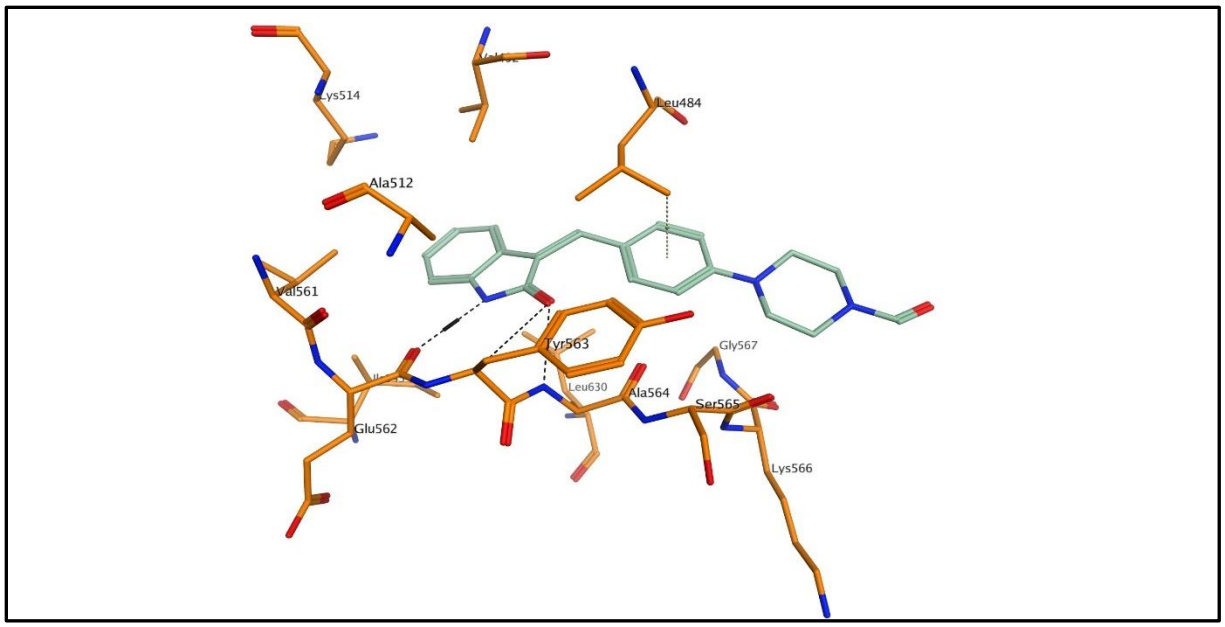

Figure S1A.

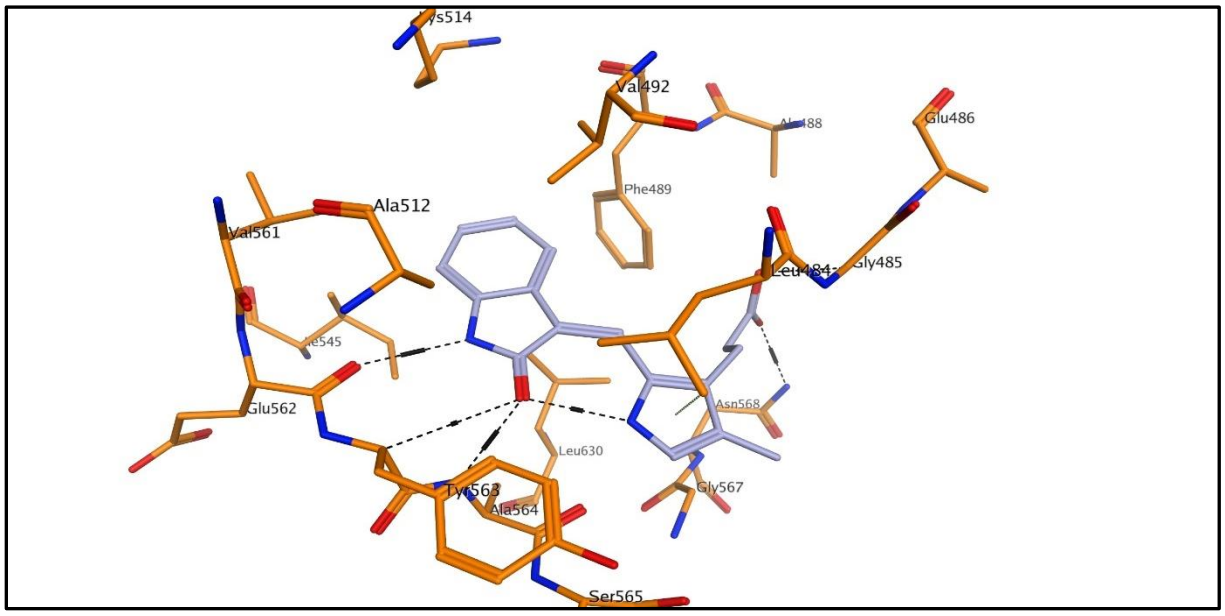

Figure S1B.

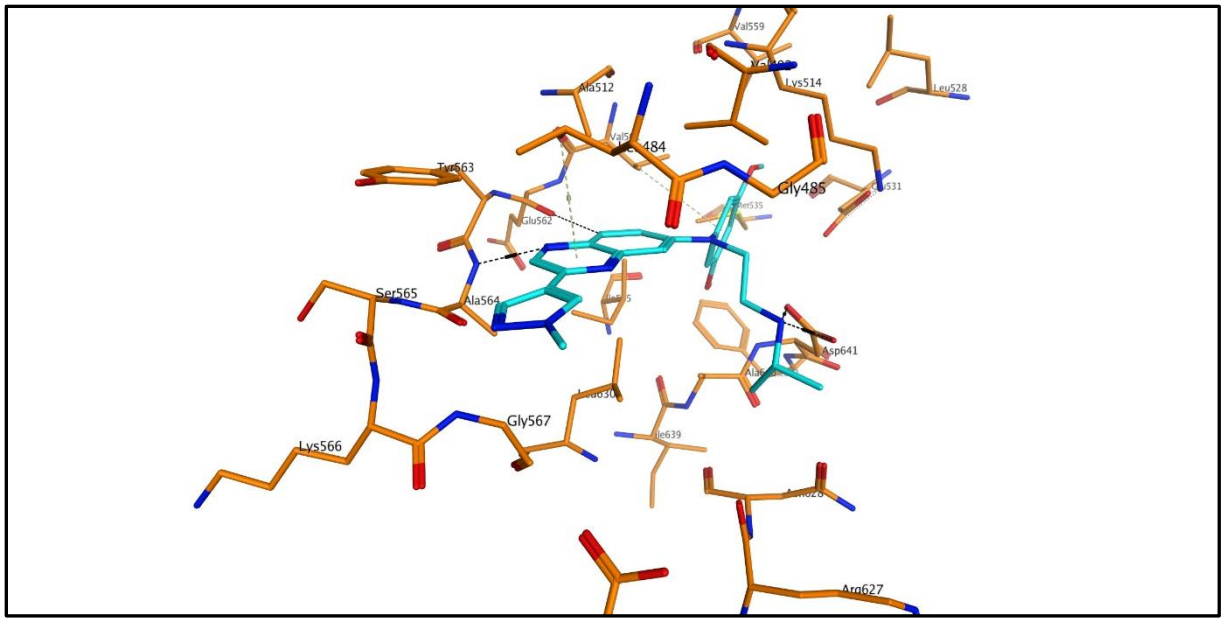

Figure S1C.

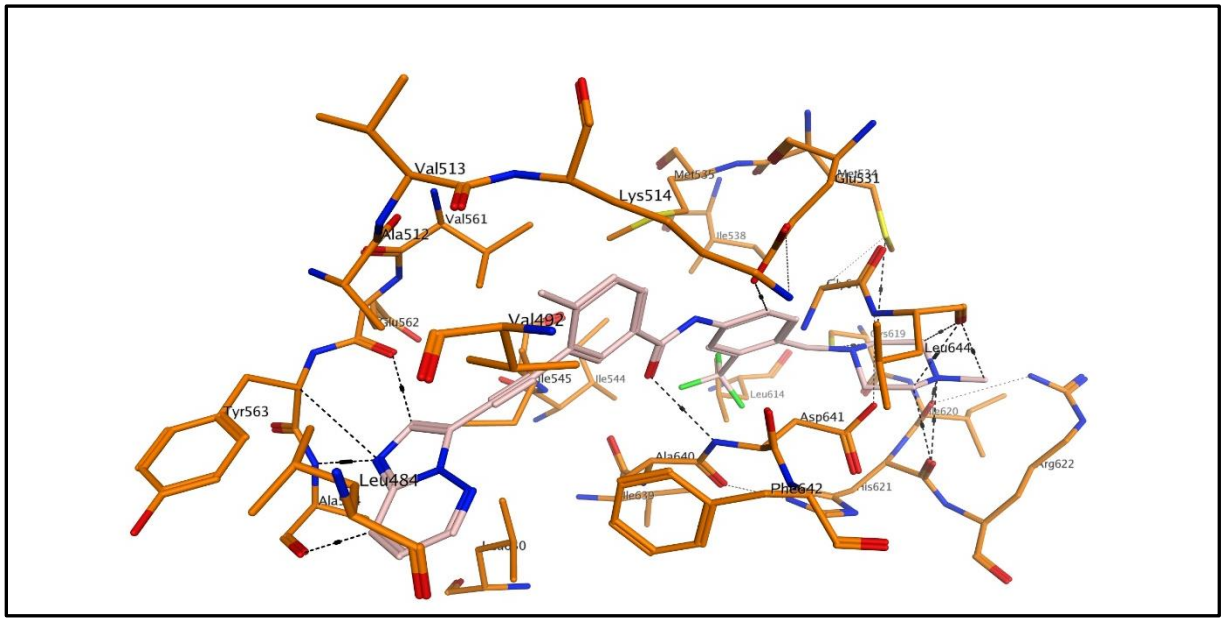

Figure S1D.

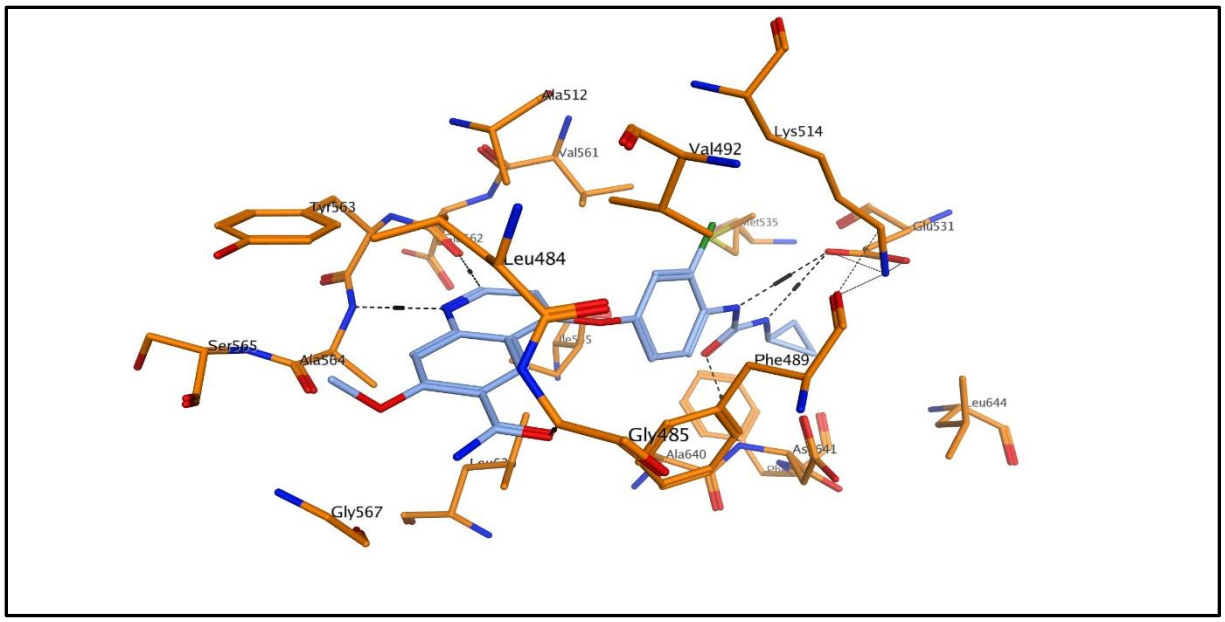

Figure S1E.

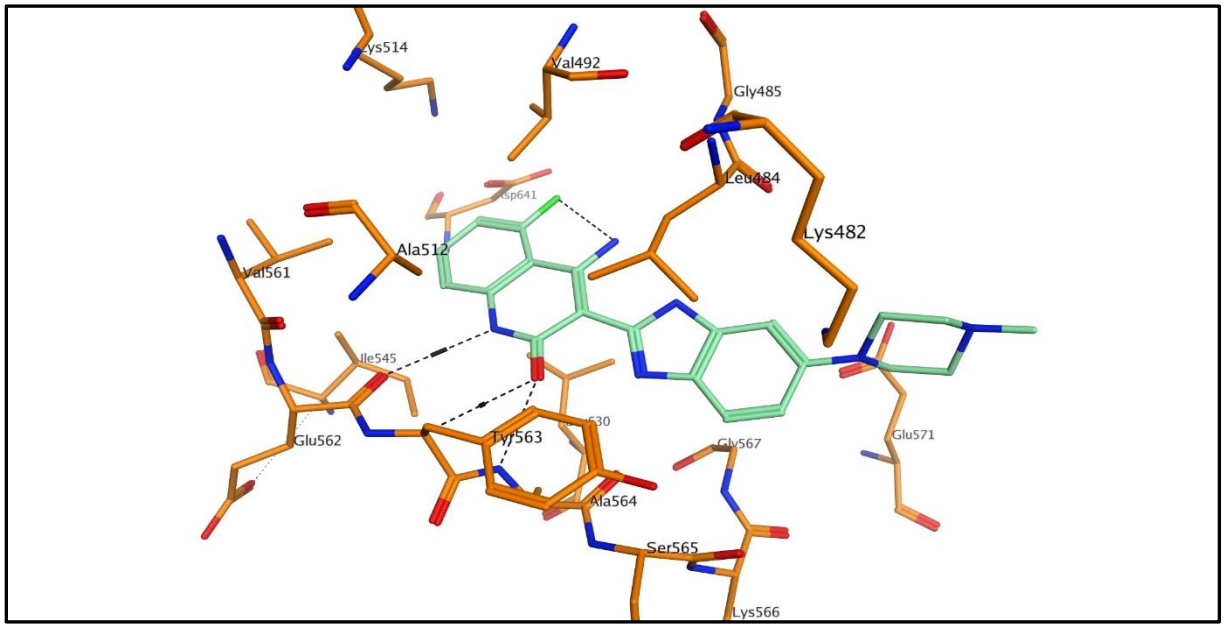

Figure S1F.

Figure S1. The binding mode of several FGFR kinase inhibitors inside the crystal structure of FGFR1. Residues are named using three letters code and specifier. For clarity, all hydrogen atoms have been ghosted. H bonds and CH-π interactions are represented by black and grey dashed lines, respectively. (A) SU4984 (Pdb id:1agw), (B) SU5402 (Pdb id:1fgi), (C) Erdafitinib (Pdb id:5ew8), (D) Ponatinib (Pdb id:4v04), (E) Lenvatinib (Pdb id:5zv2), (F) Dovatinib (Pdb id:5a46).

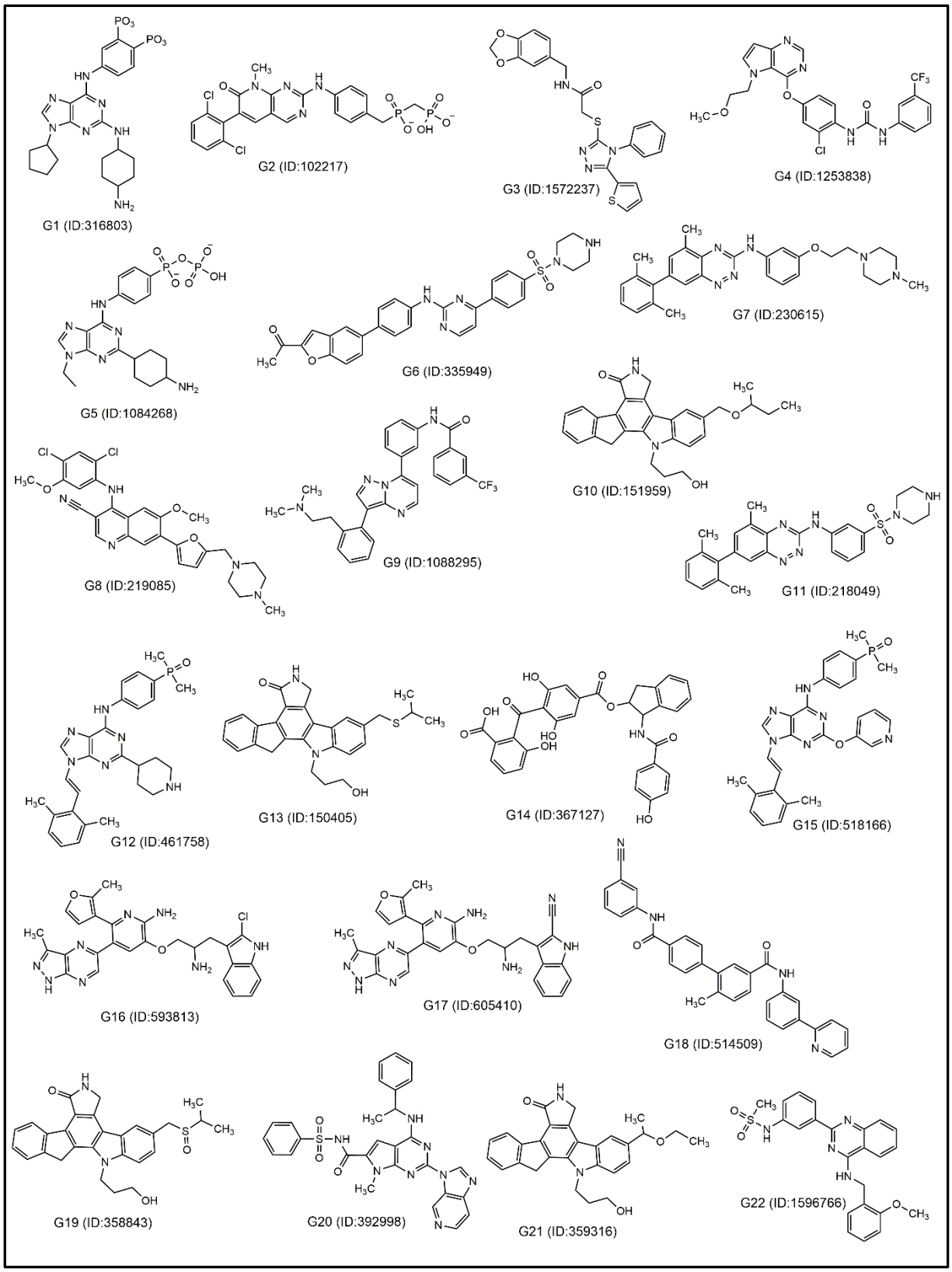

Figure S2. Chemical structures of the studied compounds with CHEMBL ID.

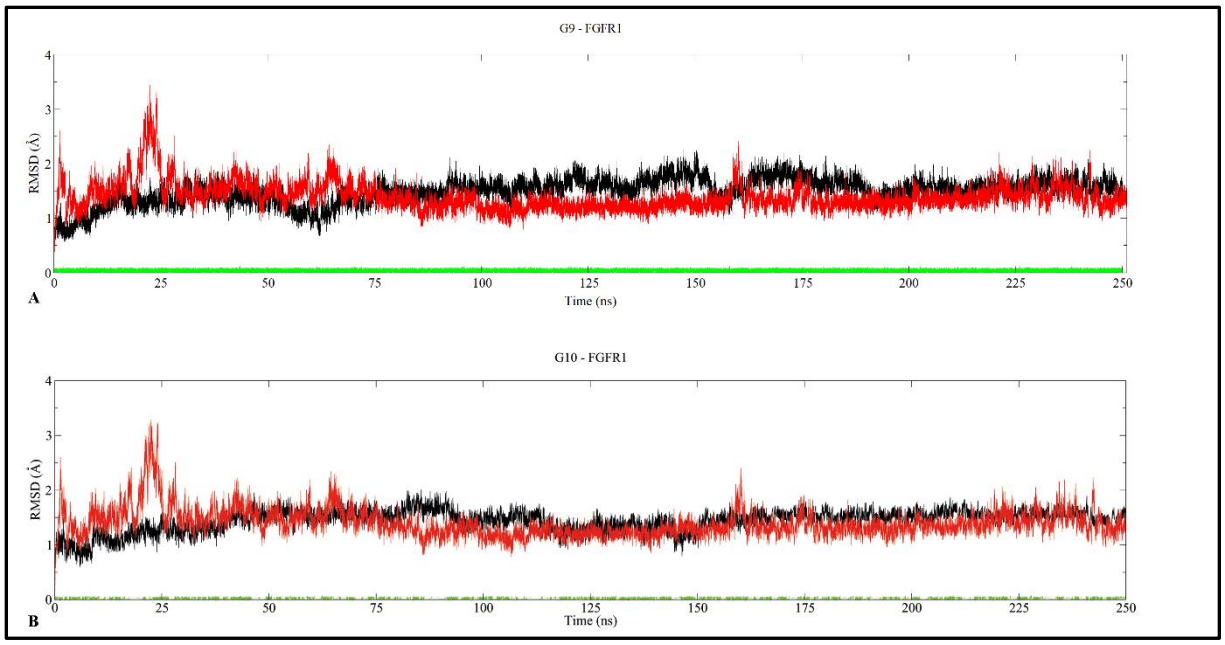

Figure S3. (A) RMSD plots of ATP-binding site residues of FGFR1 and compound **G9**-FGFR1 complex. (B) RMSD plots of ATP-binding site residues of FGFR1 and compound **G10**-FGFR1 complex. Black, red and green RMSD plots are represented for complexes, proteins and ligands, respectively.

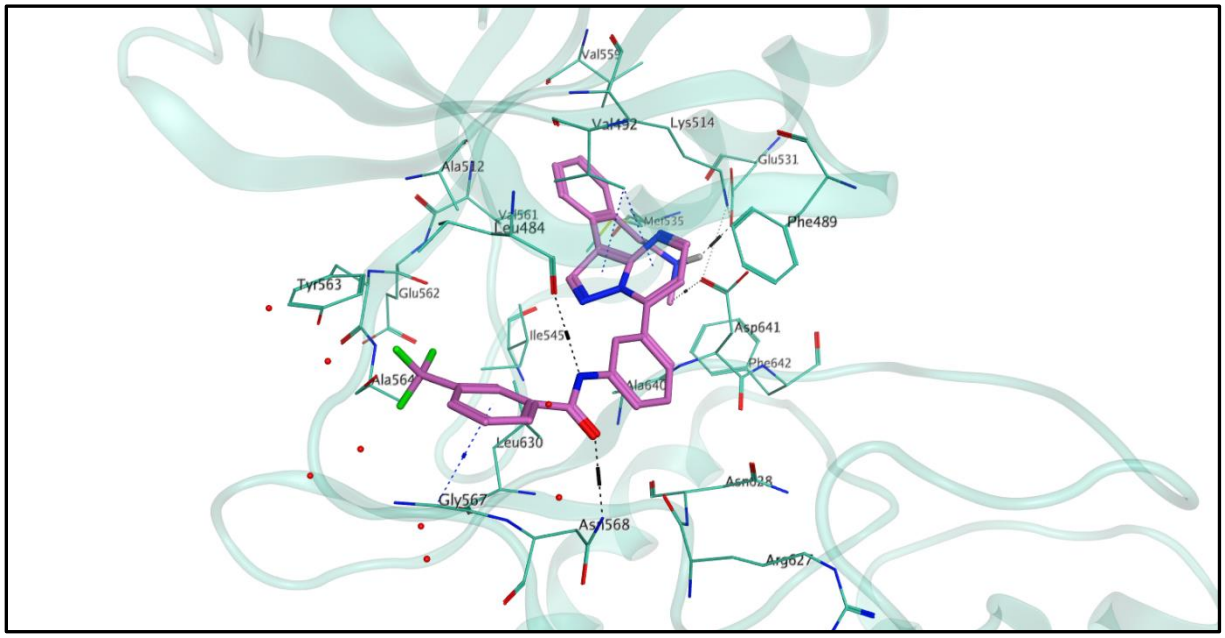

Figure S4A.

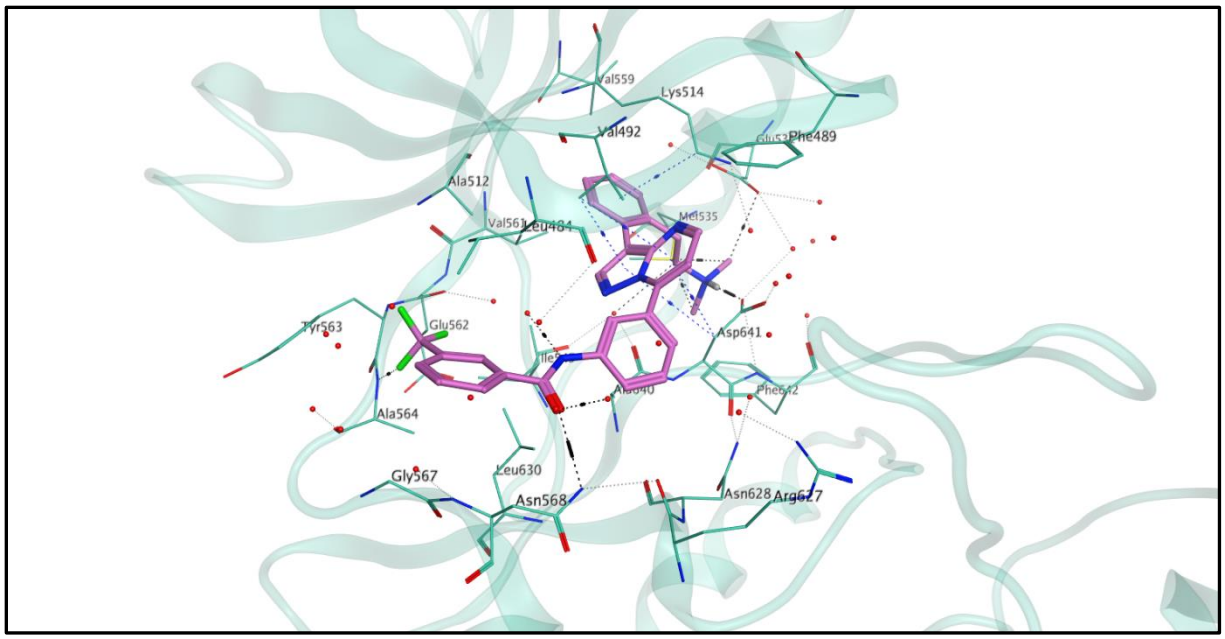

Figure S4B.

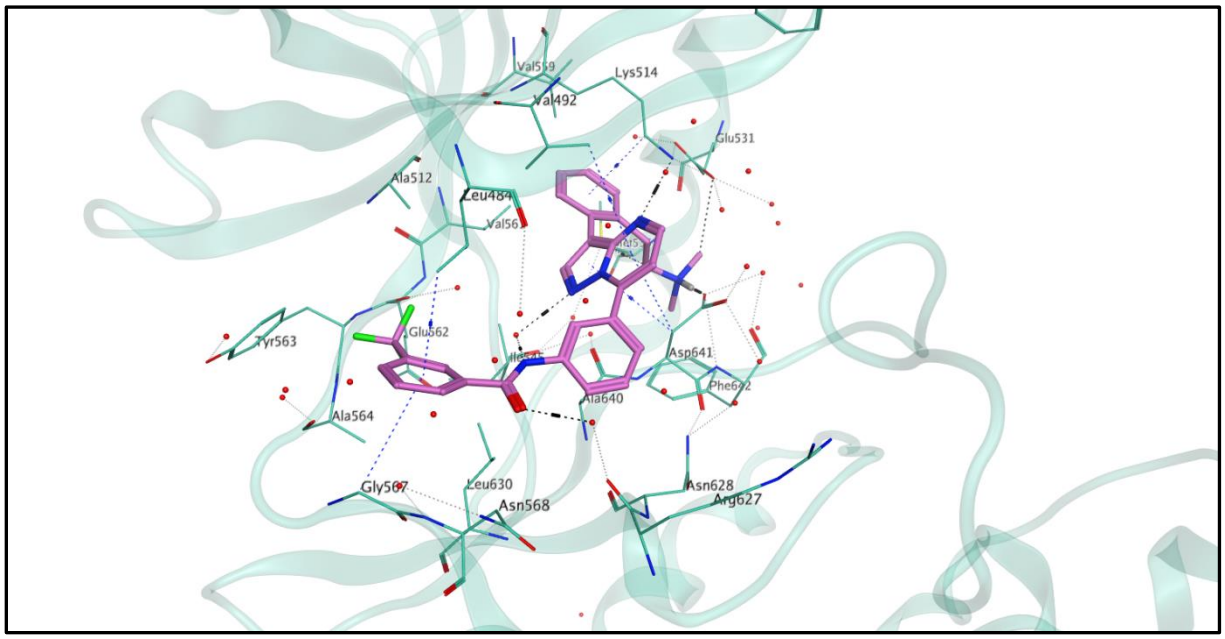

Figure S4C.

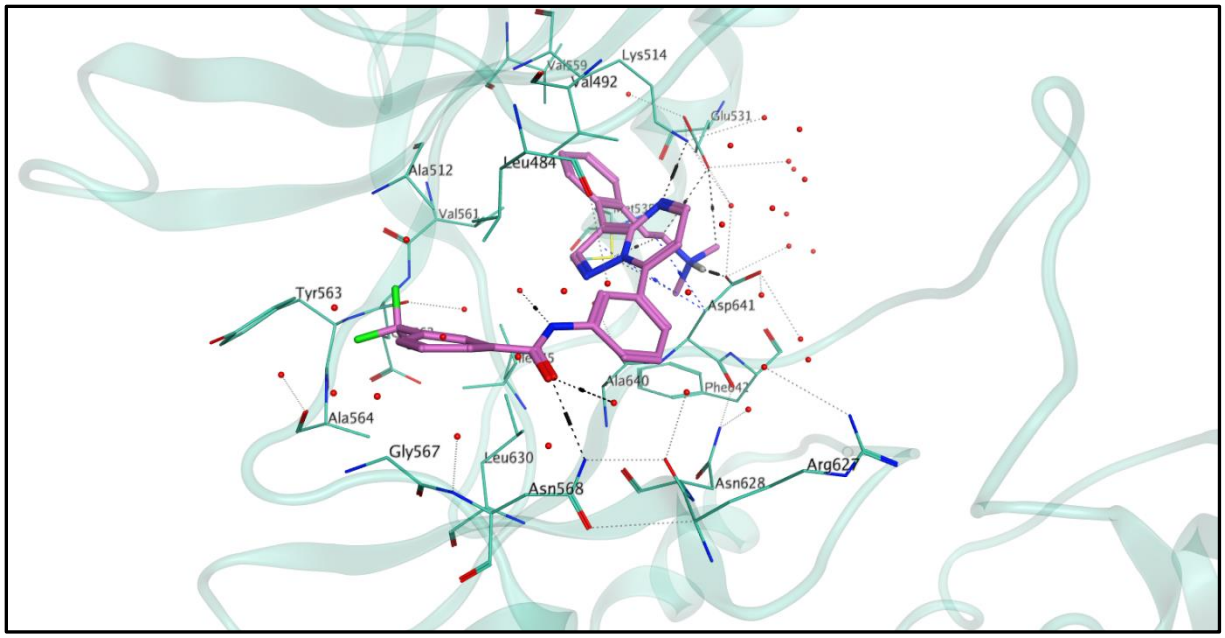

Figure S4D.

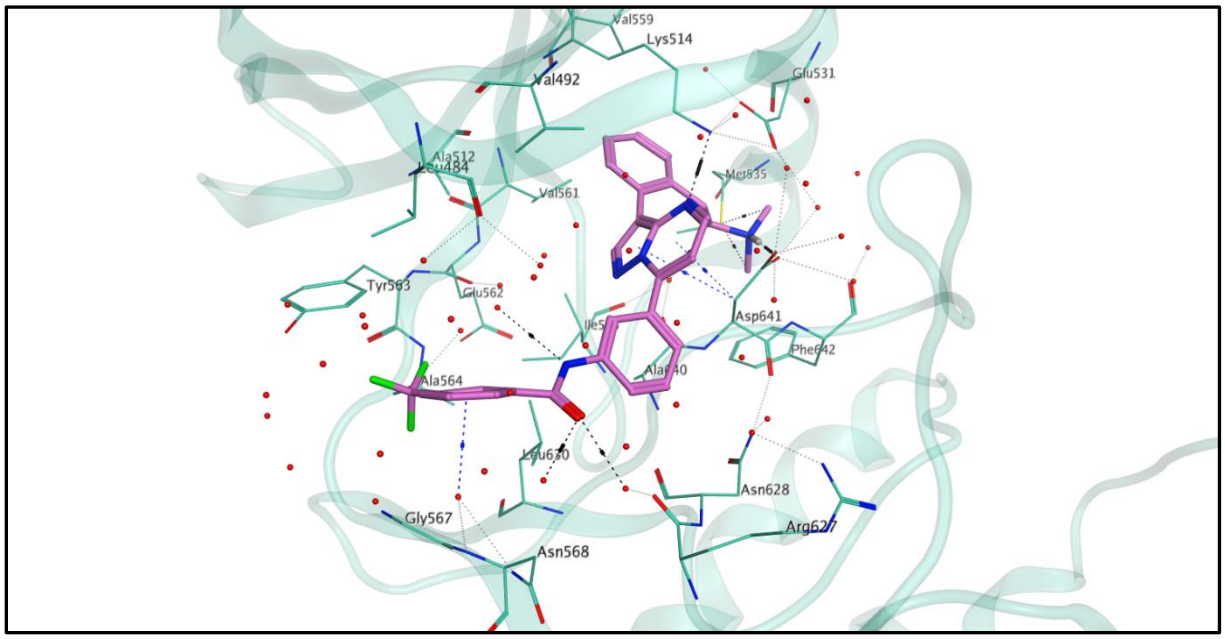

Figure S4E.

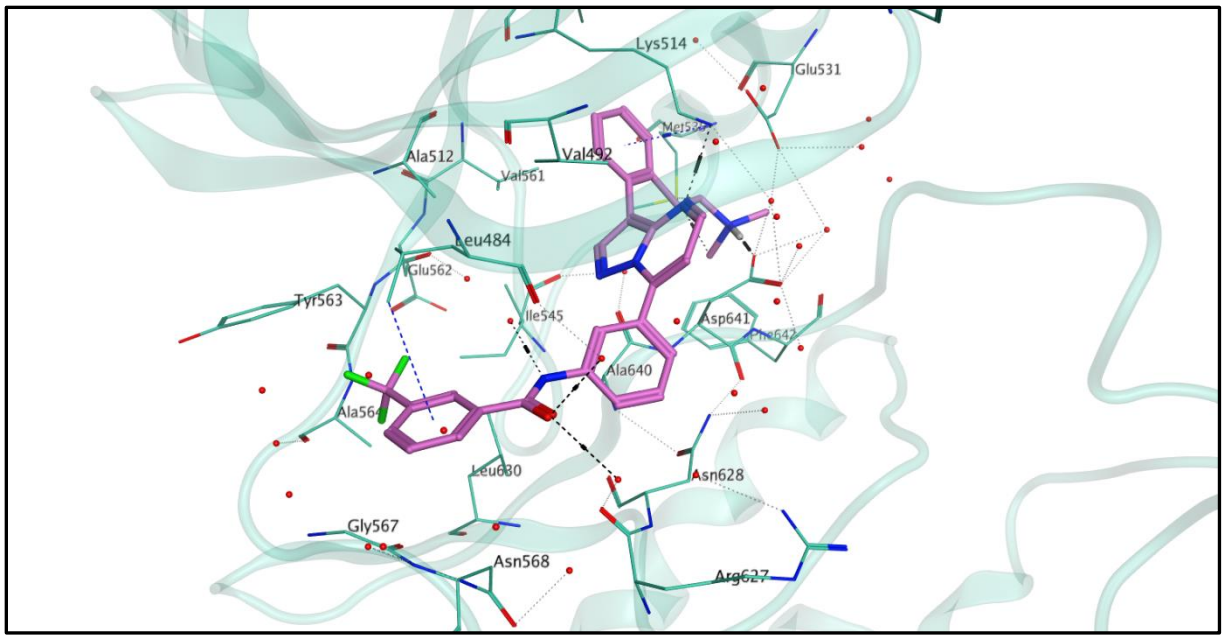

Figure S4F.

Figure S4. MD snapshots of compound **G9**-FGFR1 complex extracted from free MD simulations at 0 ns and after every 50 ns. Residues are named using three letters code and specifier. Magenta and pale cyan sticks represent compound **G9** and the active site residues, respectively. FGFR1 backbone is represented by pale cyan ribbon. For clarity, all hydrogen atoms have been ghosted. H bonds and CH-π interactions are represented by black and dark blue dashed lines, respectively. (A) at 0 ns, (B) at 50 ns, (C) at 100 ns, (D) at 150 ns, (E) at 200 ns, (F) at 250 ns.

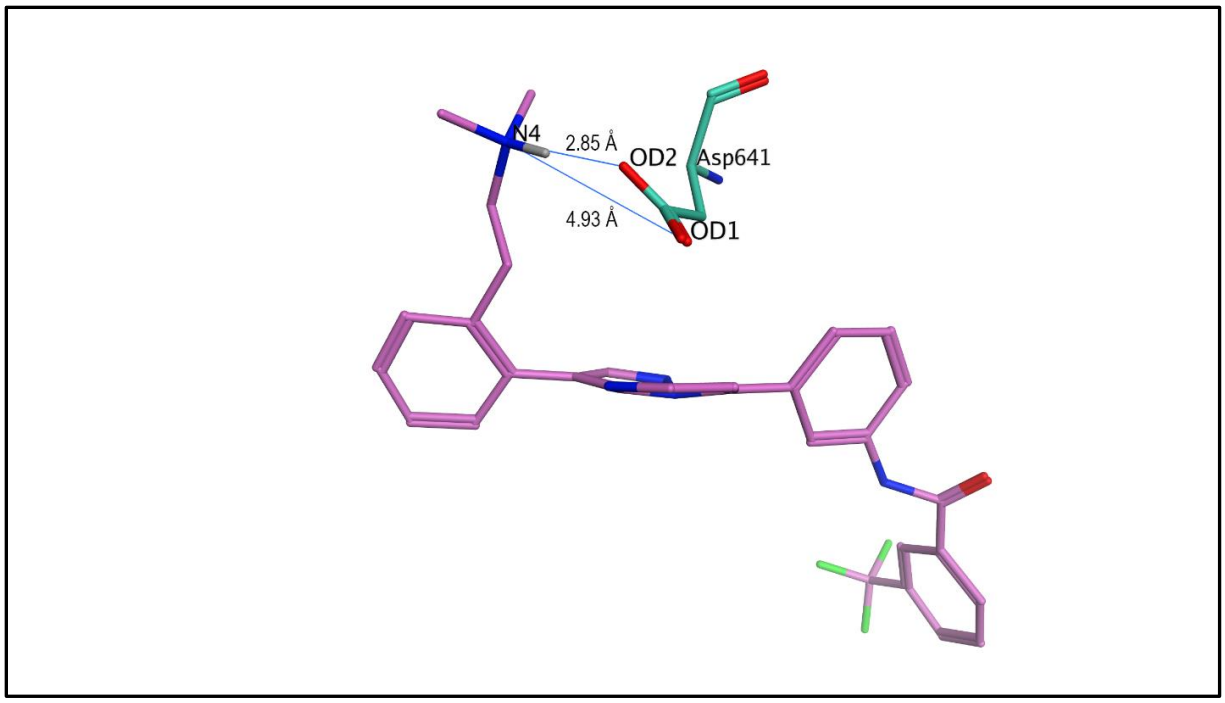

Figure S5. Atom names for Asp641 (FGFR1) and compound **G9**.

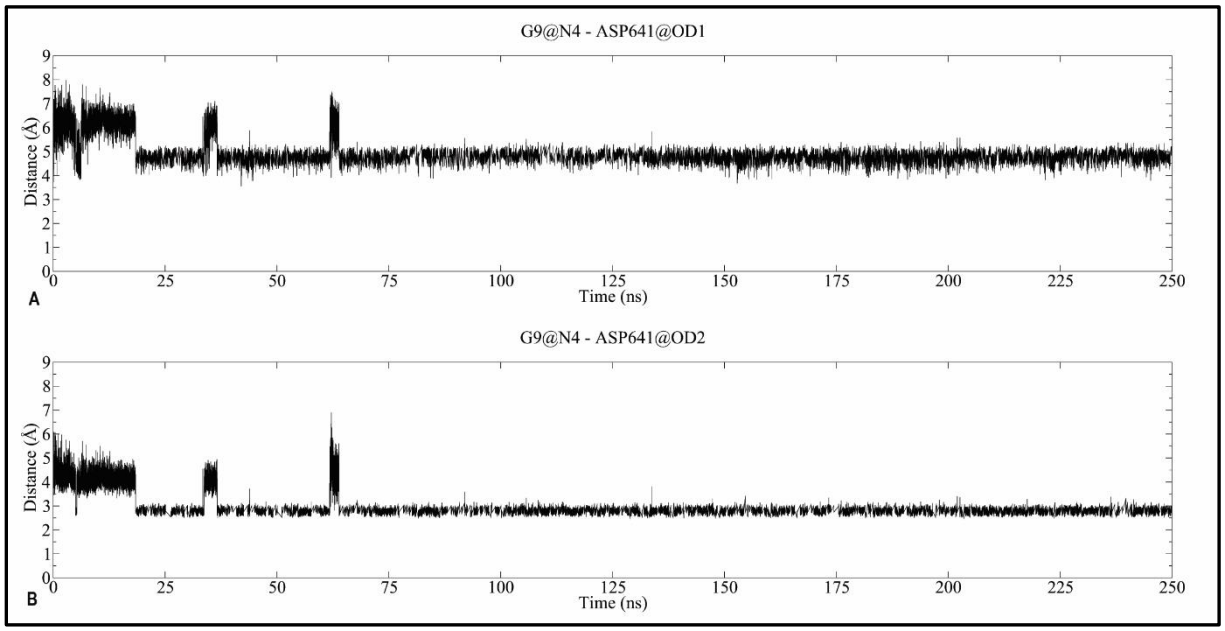

Figure S6. The plots of distances between the positively charged nitrogen of compound **G9** and oxygen atoms of carboxylate group of Asp641 of FGFR1. A) N4-641OD1 (Average Distance 4.93 Å), B) N4-641OD2 (Average Distance 2.85 Å).

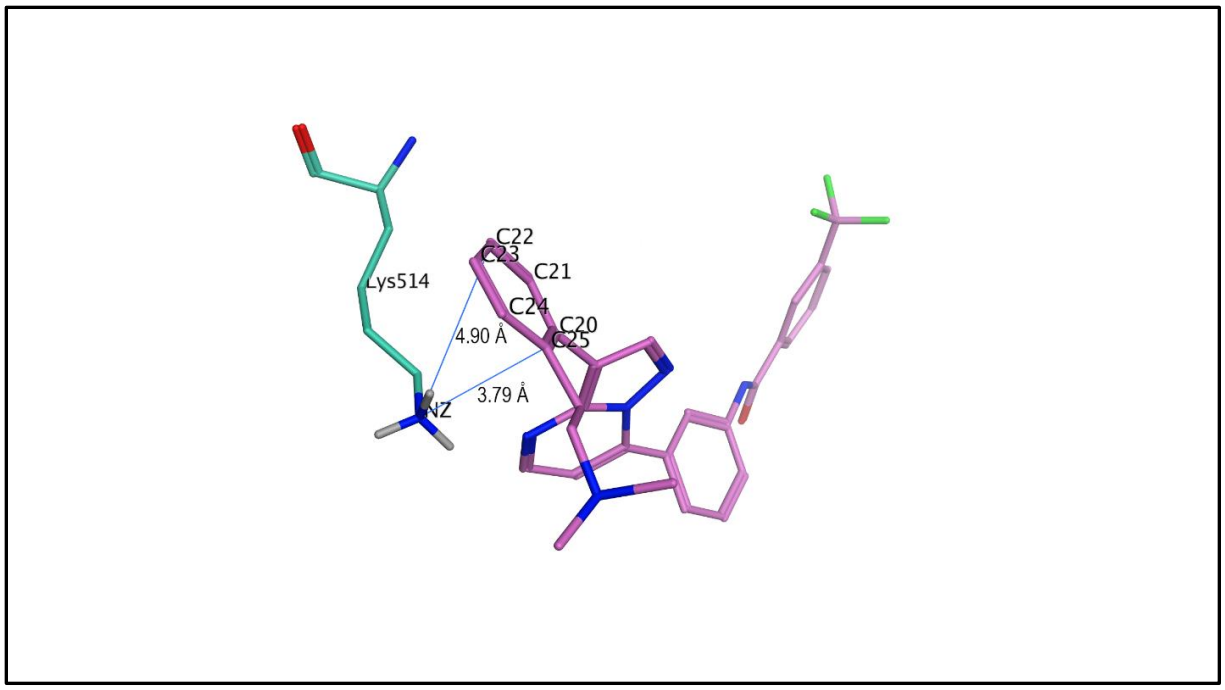

Figure S7. Atom names for Lys514 (FGFR1) and compound **G9**.

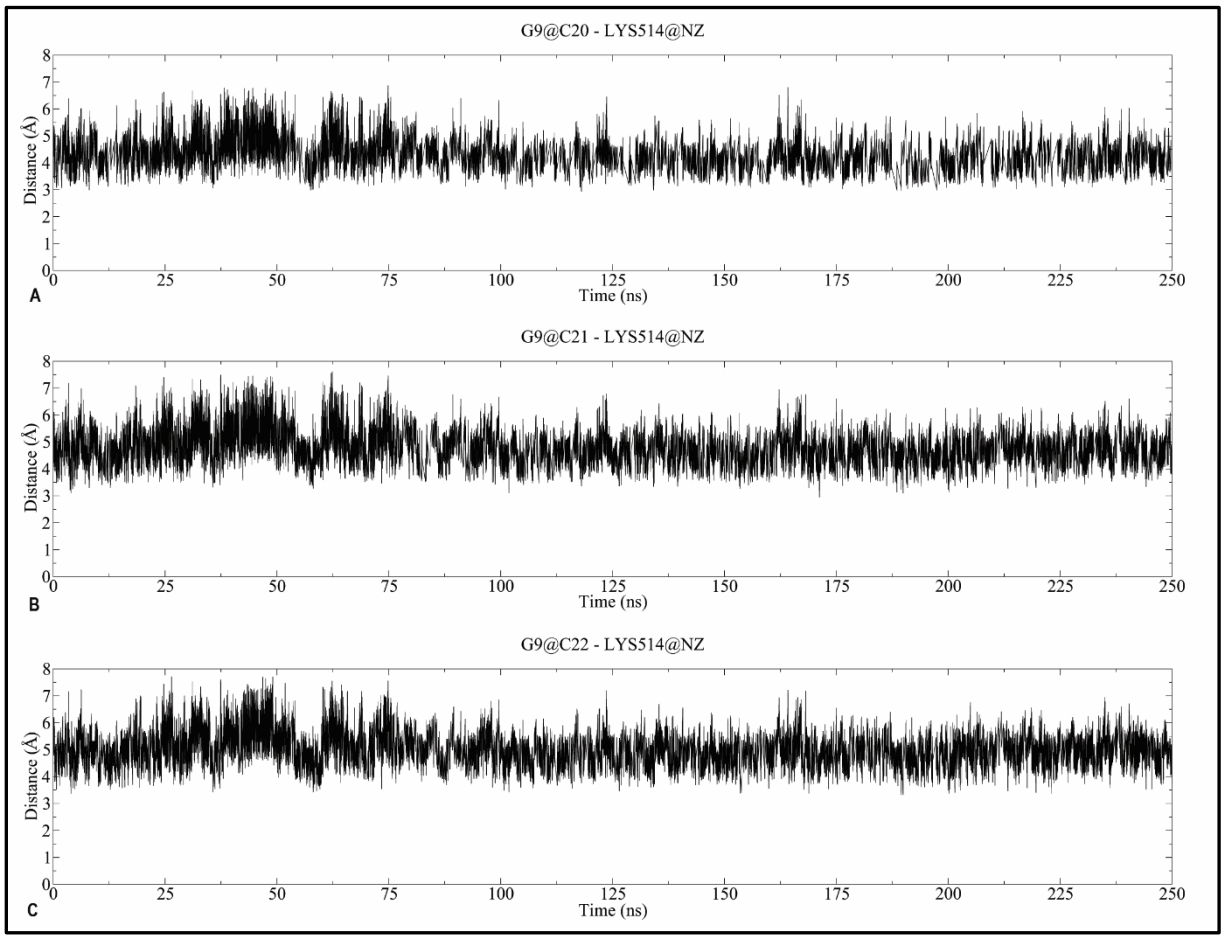

Figure S8A-S8C.

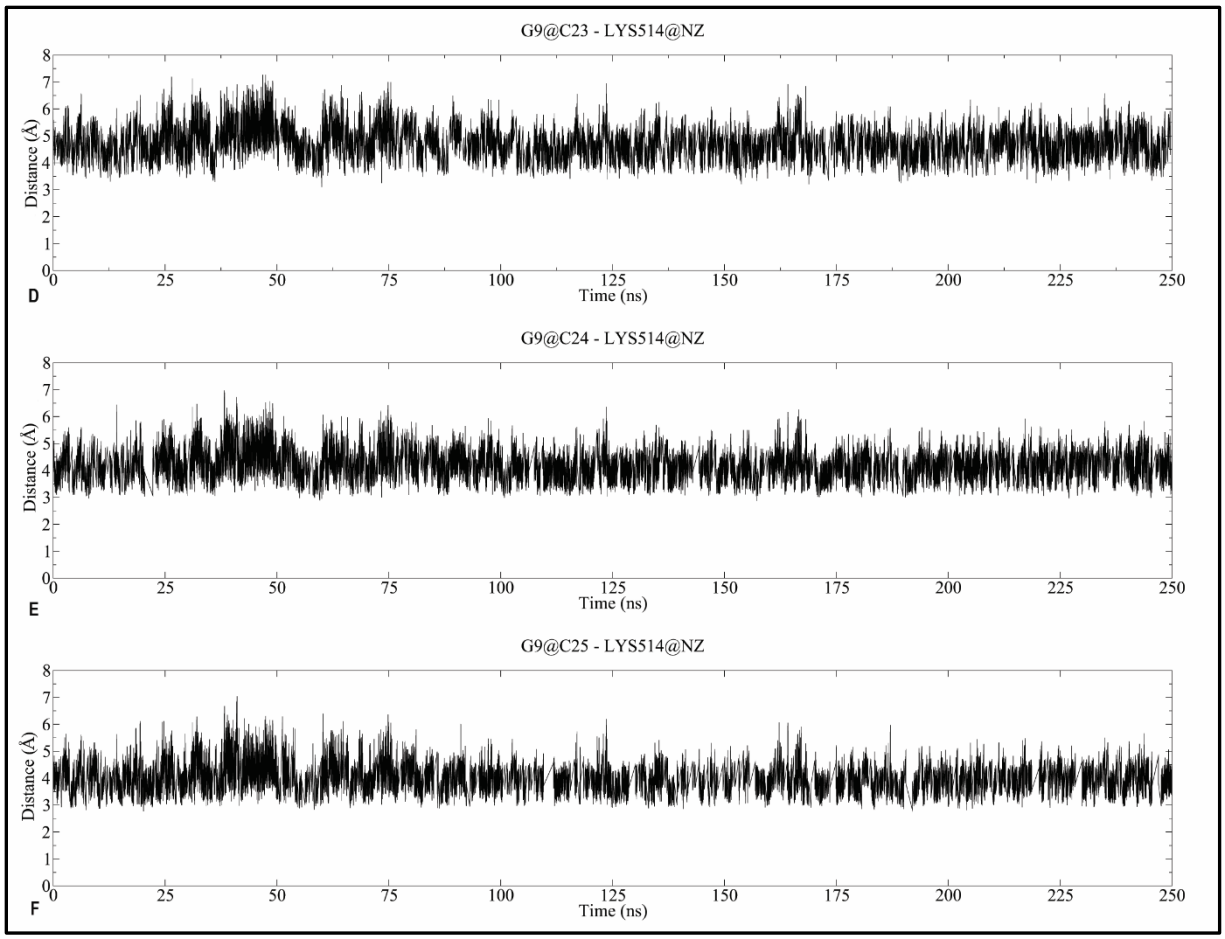

Figure S8D-S8F.

Figure S8. The plots of distances between the positively charged nitrogen of Lys514 of FGFR1 and carbon atoms of phenyl group of compound **G9**. A) 514NZ-C20 (Average Distance 4.11 Å), B) 514NZ-C21 (Average Distance 4.67 Å), C) 514NZ-C22 (Average Distance 4.90 Å), D) 514NZ-C23 (Average Distance 4.61 Å), E) 514NZ-C24 (Average Distance 4.05 Å), F) 514NZ-C25 (Average Distance 3.79 Å).

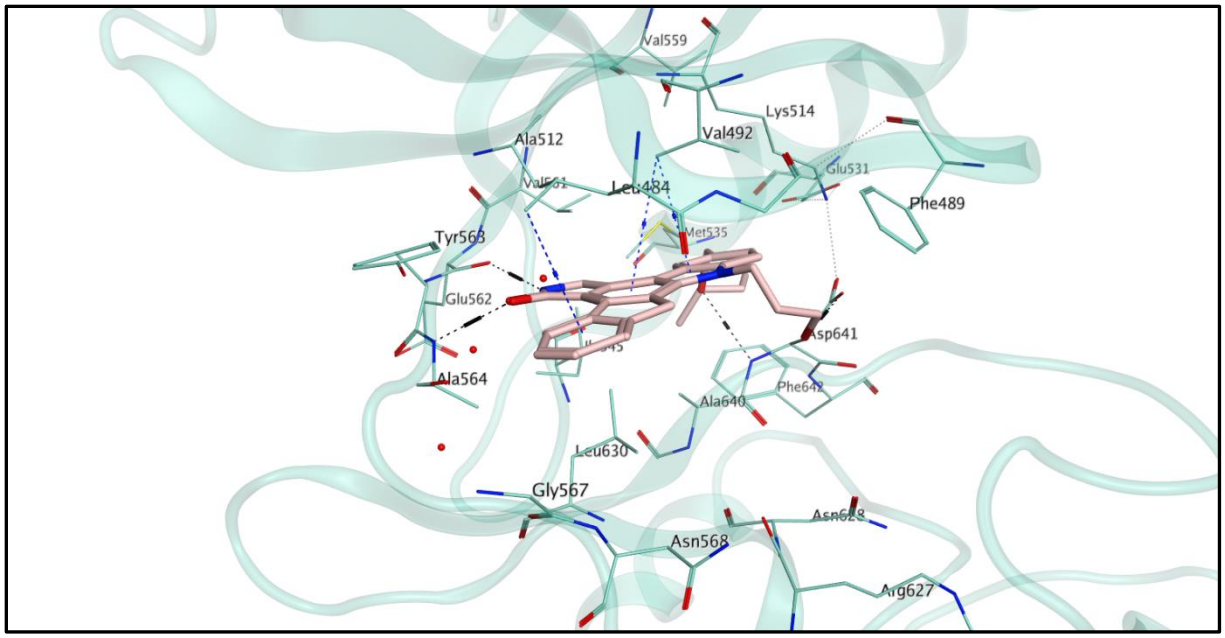

Figure S9A.

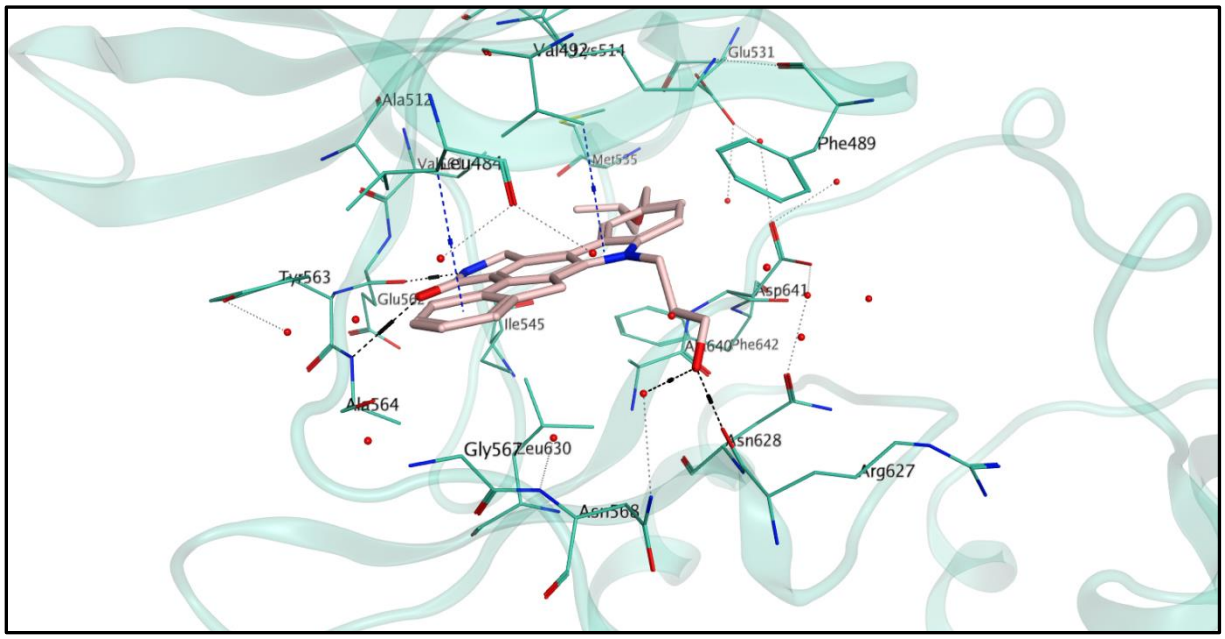

Figure S9B.

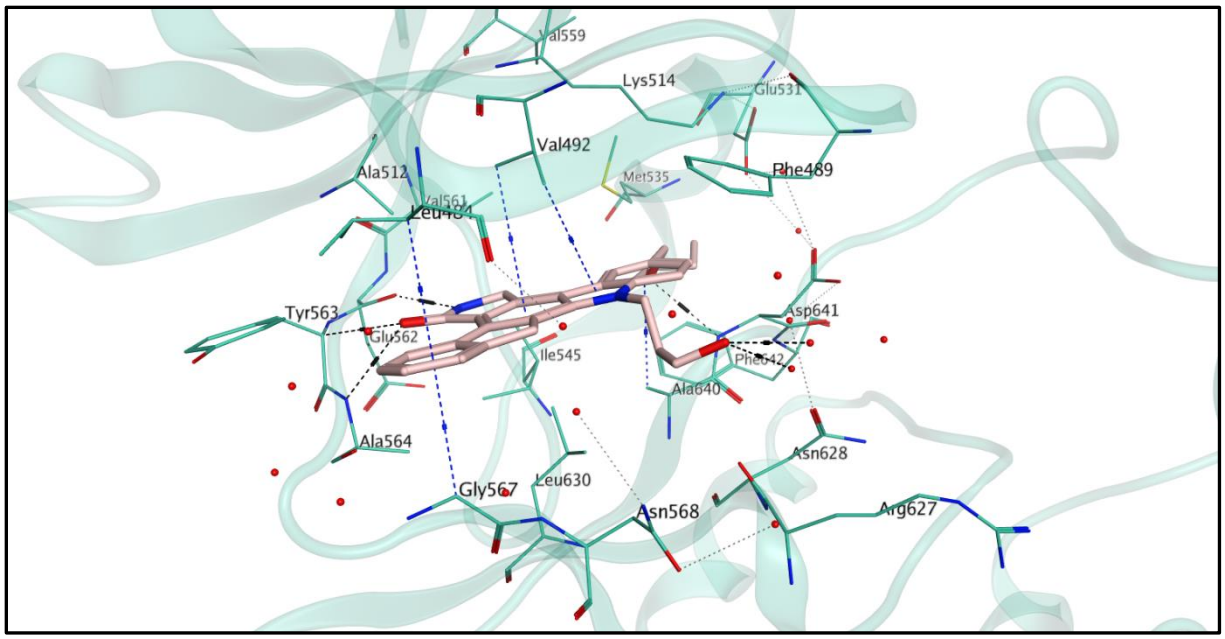

Figure S9C.

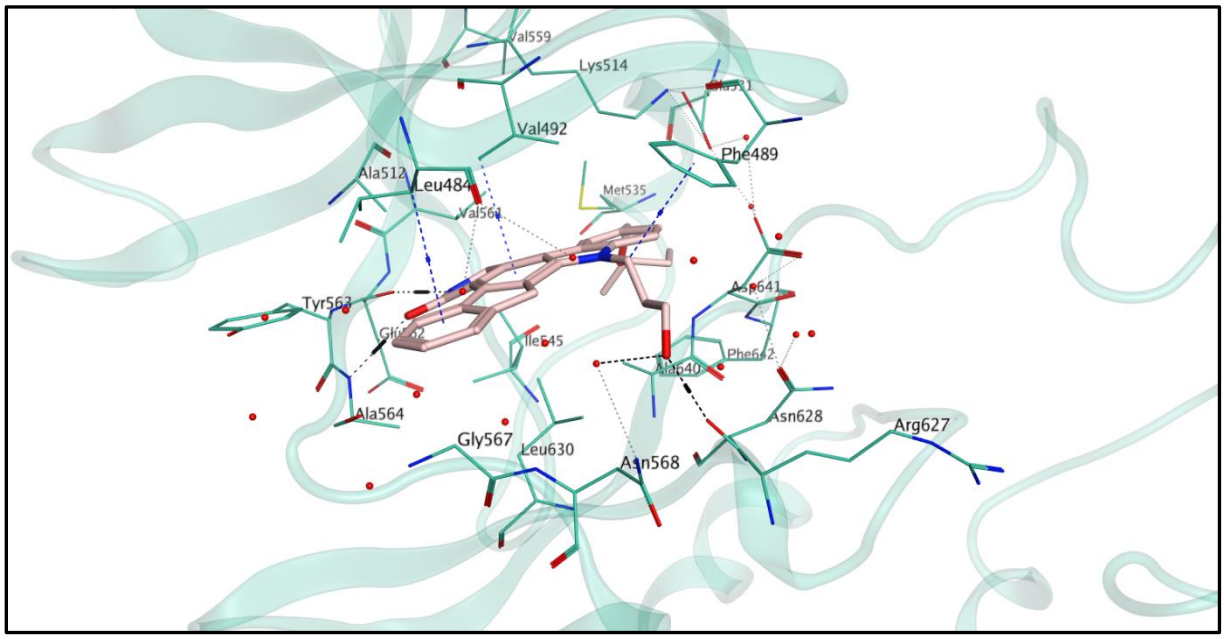

Figure S9D.

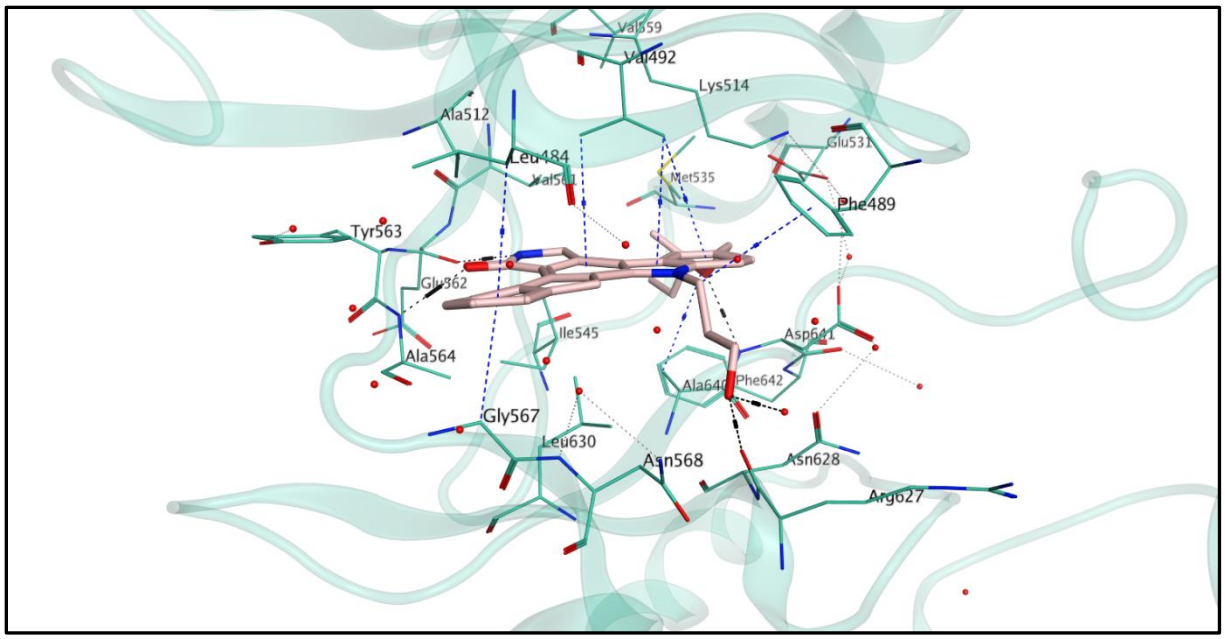

Figure S9E.

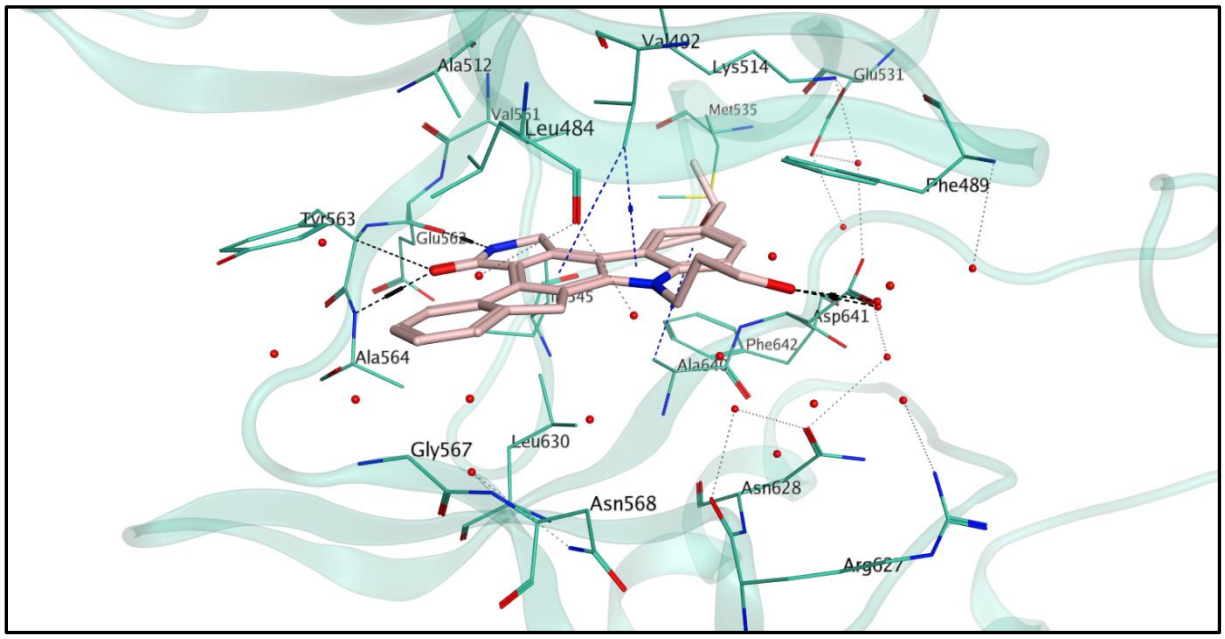

Figure S9F.

Figure S9. MD snapshots of compound **G10**-FGFR1 complex extracted from free MD simulations at 0 ns and after every 50 ns. Residues are named using three letters code and specifier. Pale pink and pale cyan sticks represent compound **G10** and the active site residues, respectively. FGFR1 backbone is represented by pale cyan ribbon. For clarity, all hydrogen atoms have been ghosted. H bonds and CH-π interactions are represented by black and dark blue dashed lines, respectively. (A) at 0 ns, (B) at 50 ns, (C) at 100 ns, (D) at 150 ns, (E) at 200 ns, (F) at 250 ns.

Table S1. Docking scores and the suggested docking poses for compounds **G1-G22** inside FGFR1 (Pdb id: 3rhx), using Goldscore.

Compound	**FGFR1**	**3D Interaction of suggested binging poses of hit**
G1 (ID:316803)	83.7928	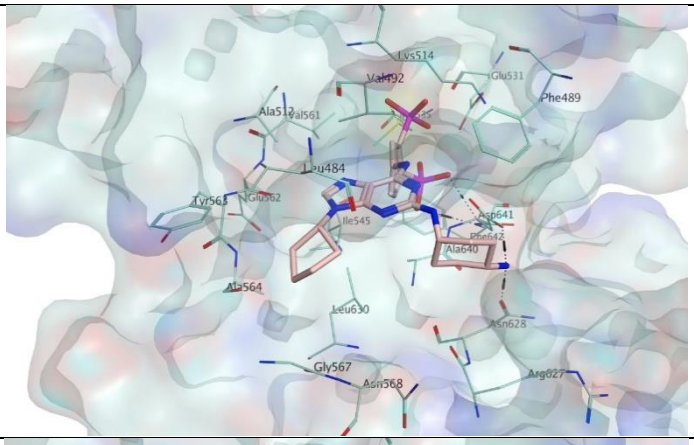
G2 (ID:102217)	83.8963	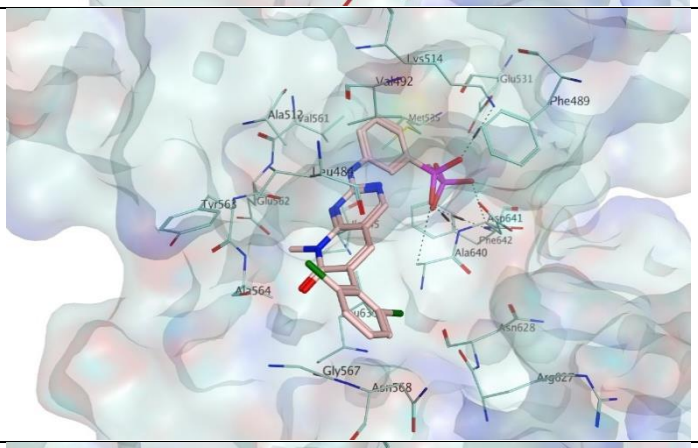
G3 (ID:1572237)	82.3749	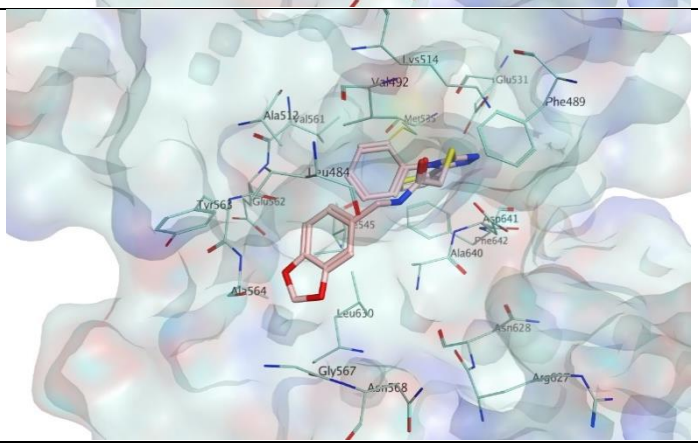

G4 (ID:1253838)	83.0826	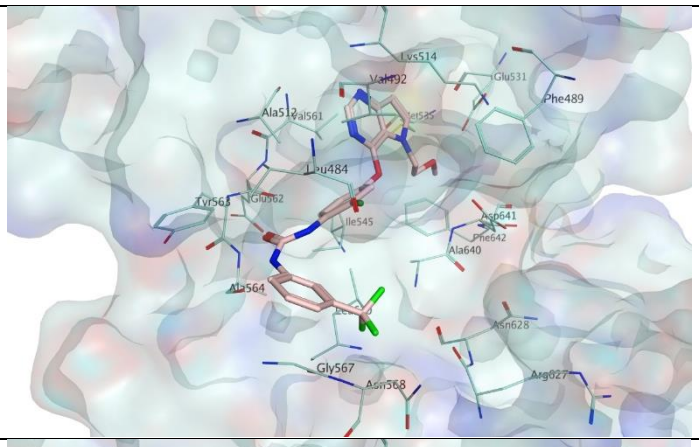
G5 (ID:1084268)	82.9231	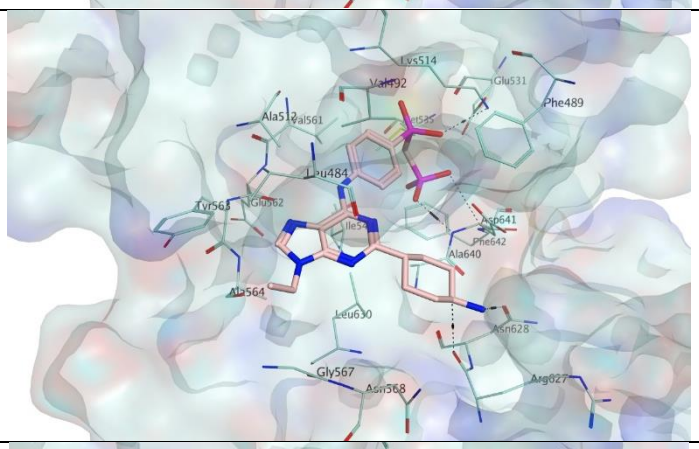
G6 (ID:335949)	84.4309	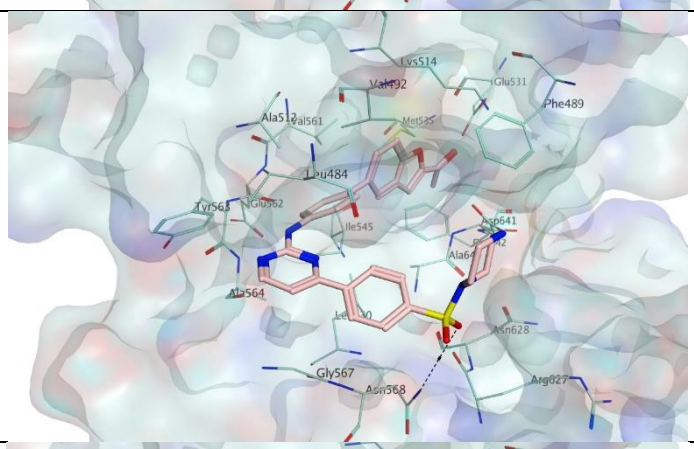
G7 (ID:230615)	82.2494	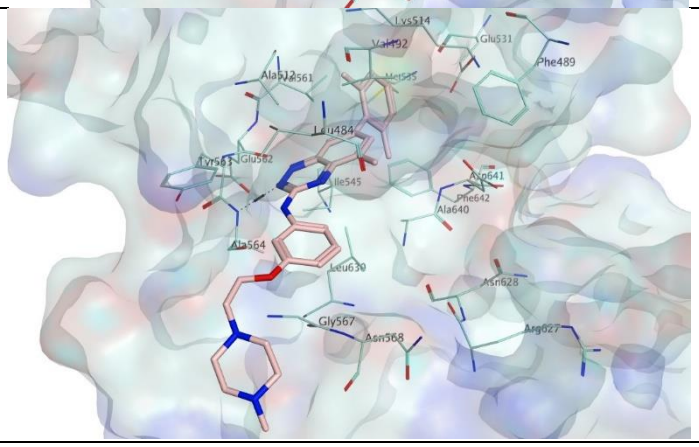

G8 (ID:219085)	80.4187	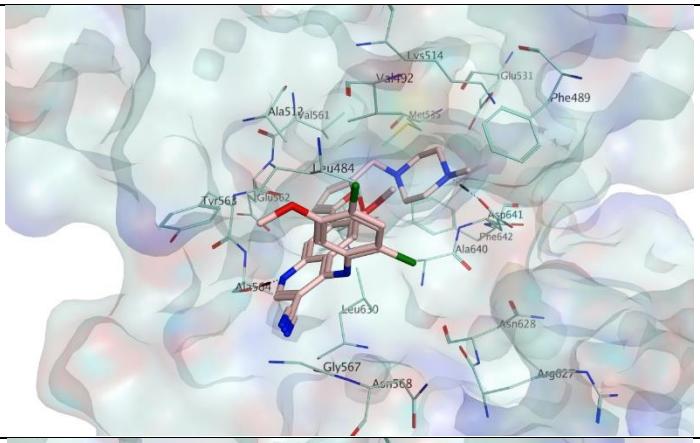
G9 (ID:1088295)	82.8773	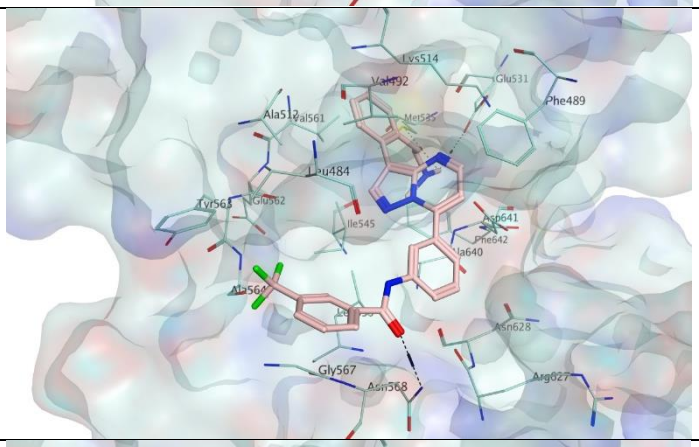
G10 (ID:151959)	82.0848	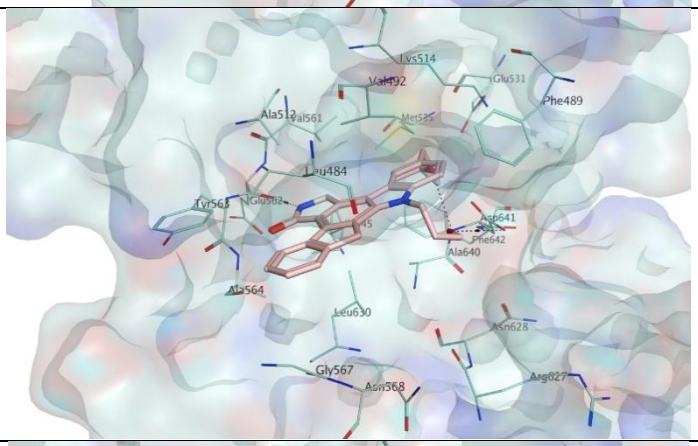
G11 (ID:218049)	81.3193	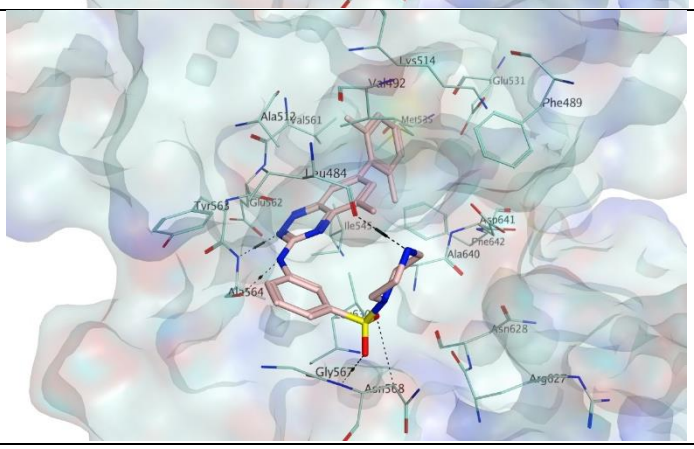

G12 (ID:461758)	81.9819	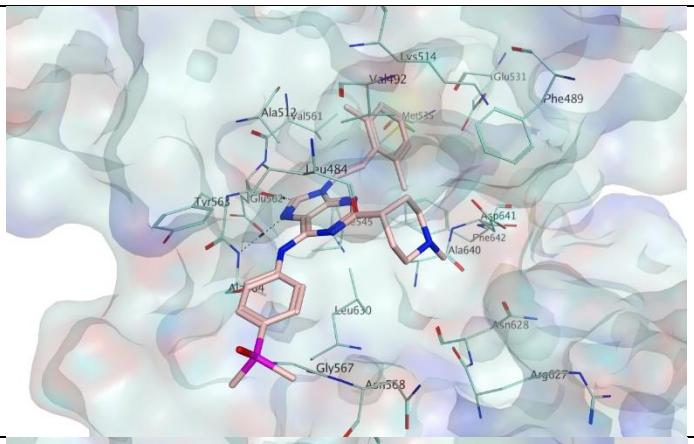
G13 (ID:150405)	84.4134	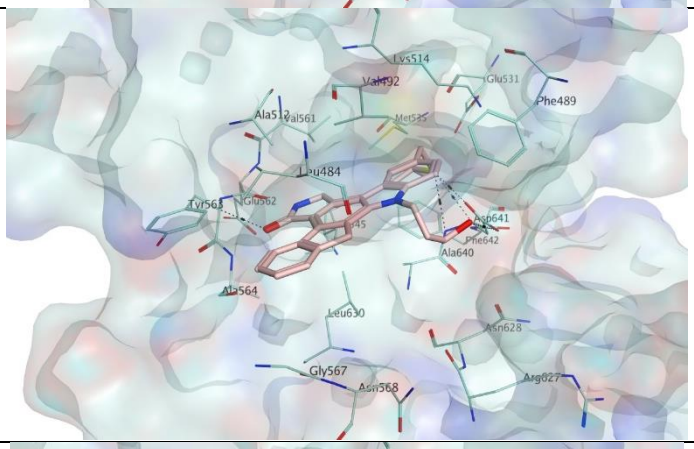
G14 (ID:367127)	84.1589	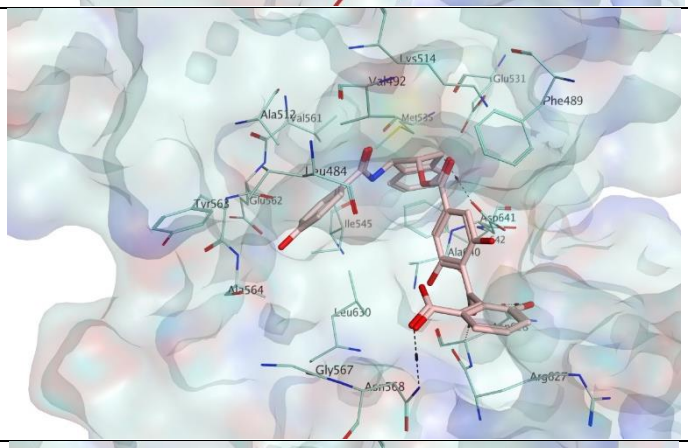
G15 (ID:518166)	83.0161	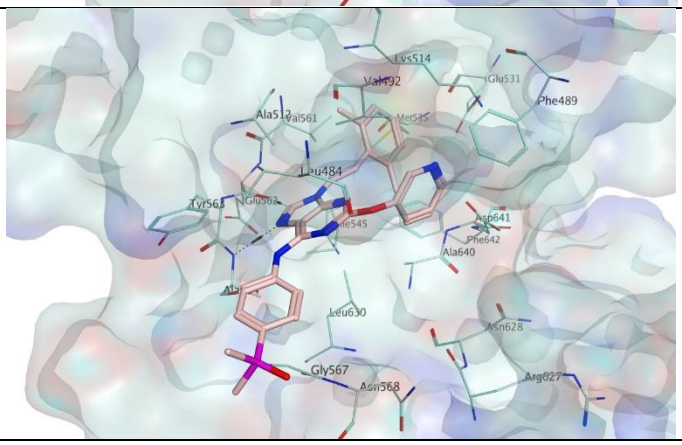

G16 (ID:593813) 85.8026	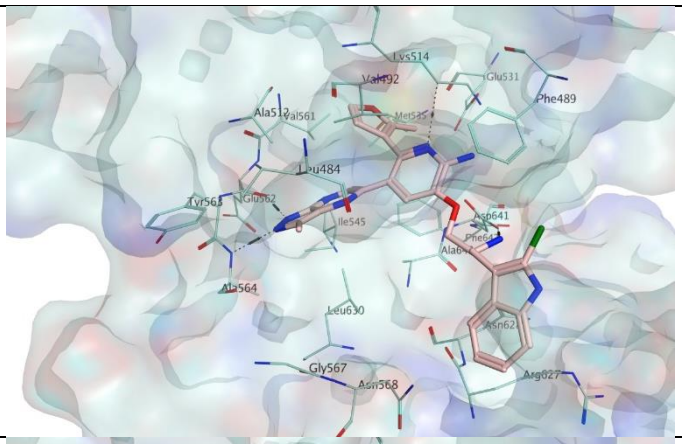
G17 (ID:605410) 83.4773	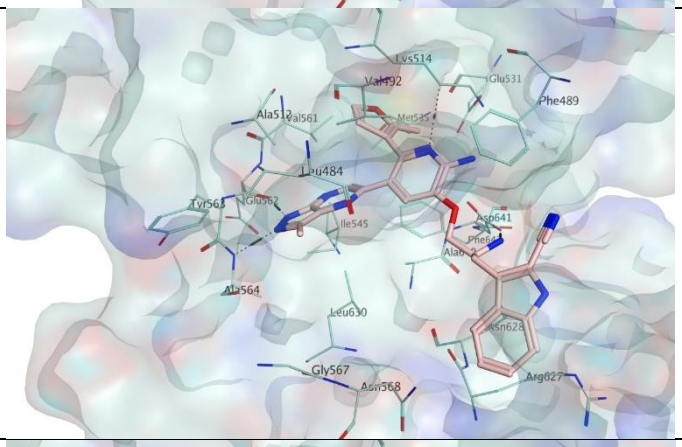
G18 (ID:514509) 83.7625	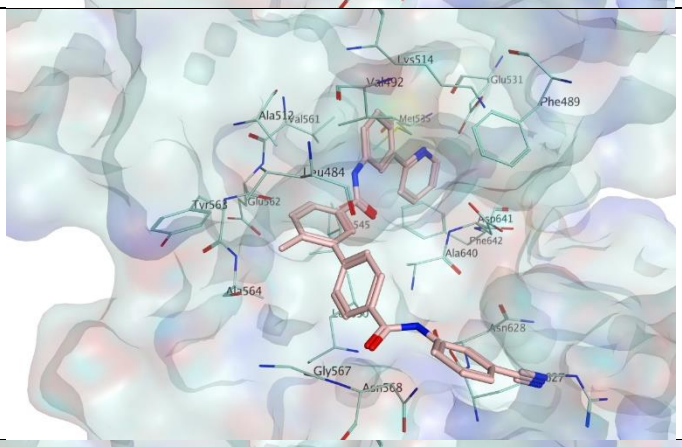
G19 (ID:358843) 82.3844	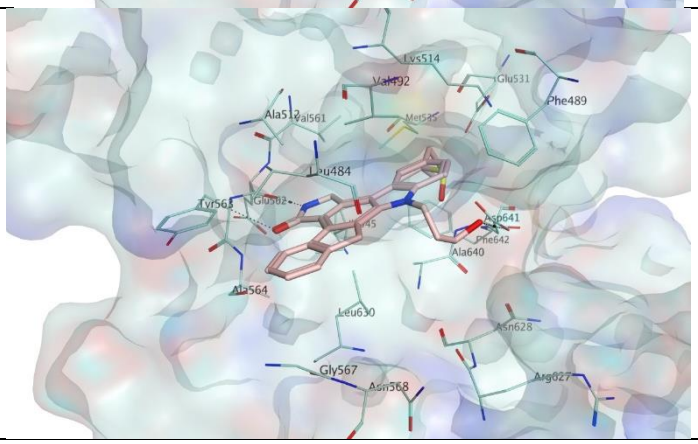

G20 (ID:392998)	81.9303	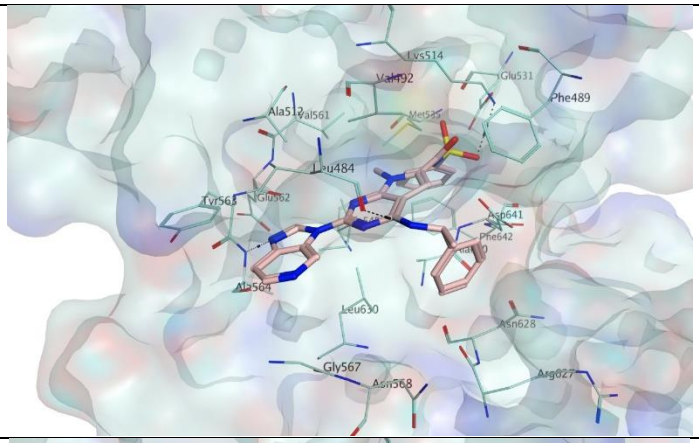
G21 (ID:359316)	80.6725	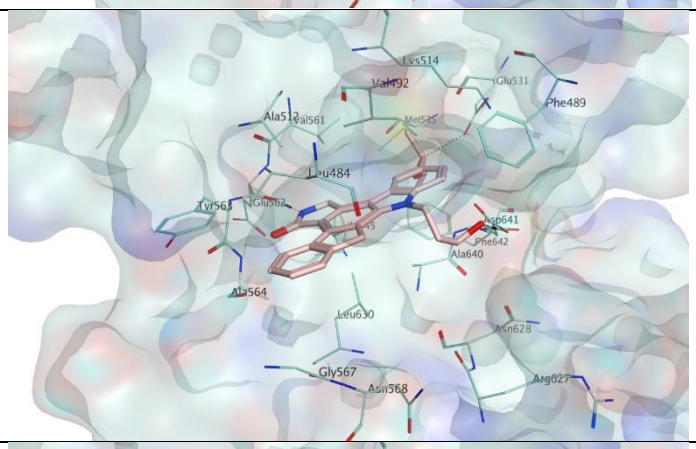
G22 (ID:1596766)	82.2491	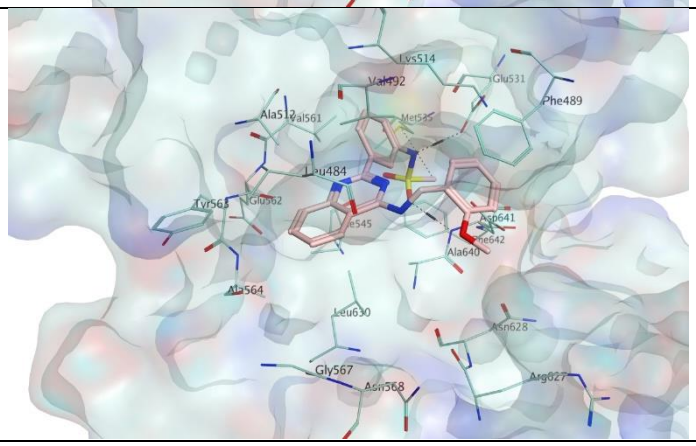

Table S2. Energy decomposition analysis energies of compound **G9** inside FGFR1 with standard errors of the mean.

Residues	Van der Waals Energy (kcal/mol)	Electrostatic Energy (kcal/mol)	Polar solvation energy (kcal/mol)	Non-polar solvation energy (kcal/mol)	Total Energy (kcal/mol)
Leu484	-2.071 +/- 0.523	0.238 +/- 0.801	-0.433 +/- 0.531	-1.700 +/- 0.349	-3.966 +/- 0.904
Val492	-1.616 +/- 0.399	0.394 +/- 0.131	-0.753 +/- 0.156	-1.150 +/- 0.246	-3.125 +/- 0.665
Lys514	-2.158 +/- 0.572	19.081 +/- 2.680	-25.715 +/- 1.595	-2.078 +/- 0.143	-10.870 +/- 1.805
Glu531	-1.936 +/- 0.490	-31.731 +/- 4.051	31.332 +/- 1.933	-1.247 +/- 0.162	-3.581 +/- 2.476
Met535	-1.677 +/- 0.329	-1.340 +/- 0.706	-0.056 +/- 0.404	-1.273 +/- 0.166	-4.347 +/- 0.651
Ile545	-0.748 +/- 0.146	-1.470 +/- 0.308	1.413 +/- 0.297	-0.373 +/- 0.113	-1.177 +/- 0.268
Val559	-0.664 +/- 0.192	-0.226 +/- 0.330	0.168 +/- 0.226	-0.587 +/- 0.075	-1.308 +/- 0.226
Val561	-1.346 +/- 0.291	0.740 +/- 0.141	-0.822 +/- 0.132	-1.229 +/- 0.111	-2.657 +/- 0.313
Tyr563	-0.830 +/- 0.322	-0.388 +/- 0.247	0.196 +/- 0.212	-0.602 +/- 0.179	-1.625 +/- 0.505
Ala564	-0.661 +/- 0.293	-0.330 +/- 0.446	0.231 +/- 0.253	-0.495 +/- 0.157	-1.256 +/- 0.523
Gly567	-0.617 +/- 0.225	0.348 +/- 0.263	-0.491 +/- 0.207	-0.530 +/- 0.157	-1.289 +/- 0.431
Asn568	-0.771 +/- 0.344	0.043 +/- 1.160	-0.877 +/- 0.373	-0.628 +/- 0.294	-2.233 +/- 1.467
Arg627	-0.519 +/- 0.133	11.900 +/- 0.743	-12.192 +/- 0.738	-0.322 +/- 0.088	-1.132 +/- 0.255
Asn628	-0.886 +/- 0.203	0.574 +/- 0.464	-0.347 +/- 0.426	-0.586 +/- 0.123	-1.245 +/- 0.280
Leu630	-1.814 +/- 0.331	0.061 +/- 0.138	-0.263 +/- 0.102	-1.413 +/- 0.176	-3.429 +/- 0.454
Asp641	-3.303 +/- 0.733	-38.026 +/- 3.130	31.971 +/- 1.265	-2.283 +/- 0.159	-11.641 +/- 2.148
Phe642	-2.073 +/- 0.438	-4.388 +/- 0.945	2.557 +/- 0.661	-1.459 +/- 0.225	-5.363 +/- 1.059

Table S3. Energy decomposition analysis energies of compound **G10** inside FGFR1 with standard errors of the mean.

Residues	Van der Waals Energy (kcal/mol)	Electrostatic Energy (kcal/mol)	Polar solvation energy (kcal/mol)	Non-polar solvation energy (kcal/mol)	Total Energy (kcal/mol)
Leu484	-2.358 +/- 0.396	-0.670 +/- 0.324	0.174 +/- 0.206	-1.692 +/- 0.229	-4.546 +/- 0.664
Phe489	-2.149 +/- 0.419	-0.331 +/- 0.203	0.352 +/- 0.166	-1.657 +/- 0.290	-3.785 +/- 0.712
Val492	-2.181 +/- 0.235	-0.247 +/- 0.092	-0.265 +/- 0.084	-1.425 +/- 0.153	-4.118 +/- 0.384
Ala512	-0.737 +/- 0.126	-0.292 +/- 0.106	0.142 +/- 0.078	-0.452 +/- 0.084	-1.339 +/- 0.198
Lys514	-1.466 +/- 0.259	1.155 +/- 0.757	-2.035 +/- 0.473	-1.117 +/- 0.168	-3.462 +/- 0.777
Glu531	-1.120 +/- 0.327	-2.344 +/- 0.709	2.343 +/- 0.496	-0.802 +/- 0.200	-1.923 +/- 0.552
Met535	-1.002 +/- 0.310	-0.007 +/- 0.117	-0.011 +/- 0.079	-1.027 +/- 0.174	-2.047 +/- 0.395
Ile545	-1.739 +/- 0.295	-0.100 +/- 0.081	-0.020 +/- 0.076	-1.414 +/- 0.170	-3.273 +/- 0.395
Val561	-0.931 +/- 0.189	0.468 +/- 0.087	-0.411 +/- 0.062	-0.819 +/- 0.162	-1.693 +/- 0.324
Glu562	-0.180 +/- 0.409	-2.468 +/- 0.692	0.364 +/- 0.371	-0.235 +/- 0.026	-2.520 +/- 0.305
Tyr563	-1.236 +/- 0.238	-2.450 +/- 0.329	0.455 +/- 0.158	-0.710 +/- 0.137	-3.941 +/- 0.460
Ala564	-0.991 +/- 0.475	-2.092 +/- 0.574	0.049 +/- 0.168	-0.868 +/- 0.114	-3.903 +/- 0.537
Gly567	-0.774 +/- 0.277	-0.458 +/- 0.291	-0.205 +/- 0.165	-0.664 +/- 0.166	-2.101 +/- 0.575
Asn568	-0.962 +/- 0.377	-0.670 +/- 1.133	-0.436 +/- 0.324	-0.802 +/- 0.304	-2.869 +/- 1.460
Arg627	-0.264 +/- 0.545	-1.124 +/- 1.647	-0.066 +/- 0.708	-0.435 +/- 0.199	-1.889 +/- 0.999
Asn628	-0.627 +/- 0.344	-0.949 +/- 0.971	0.341 +/- 0.446	-0.409 +/- 0.201	-1.643 +/- 0.872
Leu630	-2.580 +/- 0.419	-0.374 +/- 0.104	0.063 +/- 0.093	-1.689 +/- 0.223	-4.580 +/- 0.608
Ala640	-1.720 +/- 0.294	-1.167 +/- 0.249	-0.493 +/- 0.145	-1.044 +/- 0.191	-4.424 +/- 0.727
Asp641	-2.178 +/- 0.421	-3.111 +/- 0.877	1.898 +/- 0.765	-1.542 +/- 0.176	-4.934 +/- 0.665
Phe642	-1.581 +/- 0.389	-0.075 +/- 0.103	0.216 +/- 0.077	-1.204 +/- 0.263	-2.645 +/- 0.588

Database Preparation and Docking Validation Protocol

The studied database was taken from ChEMBL KinaseSARfari database (ftp://ftp.ebi.ac.uk/pub/databases/chembl/KinaseSARfari/releases/5.01). The compounds, which have a molecular weight under 250 and over 650 and /or bearing the groups are able to form covalent bonding, were eliminated. The reason of a threshold value of molecular weight was selected between 250 and 650 is the FDA approved kinase inhibitors have molecular weight with a range of 306 (ruxolitinib) to 615 (trametinib).

Before the docking study of the studied compounds, in order to validate docking methods, erdafitinib as well-known FDA approved selective FGFR inhibitor, and the FDA approved kinase inhibitors as lenvatinib, and phase 3 stage compound as dovitinib, and selective FGFR inhibitor as AZD4547 were exposed to dock inside the ATP binding site of FGFR1 (PDB id: 3rhx). The best ranked docking poses of these inhibitors inside the prepared structure were superimposed with the crystal structures of inhibitor-FGFR1 complexes (PDB id: 5ew8, 5zv2, 5a46, 4v05). For instance, the superimpositions of the crystal structure of erdafinitinib-FGFR1 complex (PDB id: 5ew8.pdb) and AZD4547-FGFR1 complex (PDB id: 4v05.pdb) with the best ranked docking poses of erdafinitinib and AZD4547 inside the prepared structure of FGFR1 (3RHX) were figured in Figure S10 and Figure S11, respectively. The best ranked docking poses and the scoring values of these inhibitors inside prepared FGFR were figured and reported in Table S4. The calculated docking scores of FGFR inhibitors inside FGFR1 were observed between value as 63.97 and 85.75. Therefore, a threshold value of GoldScore fitness as 70 for virtual screening and 80 for docking study, respectively, were applied, the compounds which have GoldScore fitness value lower than these values, were gradually eliminated.

Determining MM-GBSA free binding energy threshold value

Regarding the chosen as a threshold value of MM-GBSA as -50 Kcal/mole, it was decided after the calculated MM-GBSA free binding energy values for erdafitinib and AZD4547 inside FGFR1 from 10 ns MDS. First ranked docking poses of these inhibitors inside FGFR1 were used as initial structures of generated MDS. Free binding energies were calculated as -56.5209 Kcal/mole for erdafitinib in FGFR1 and -46.8109 Kcal/mole for AZD4547 in FGFR1. MM-GBSA calculation results for these inhibitors were given in Table S5. Therefore, the threshold value of MM-GBSA as -50 Kcal/mole was determined because of the fact that between these two calculated values.

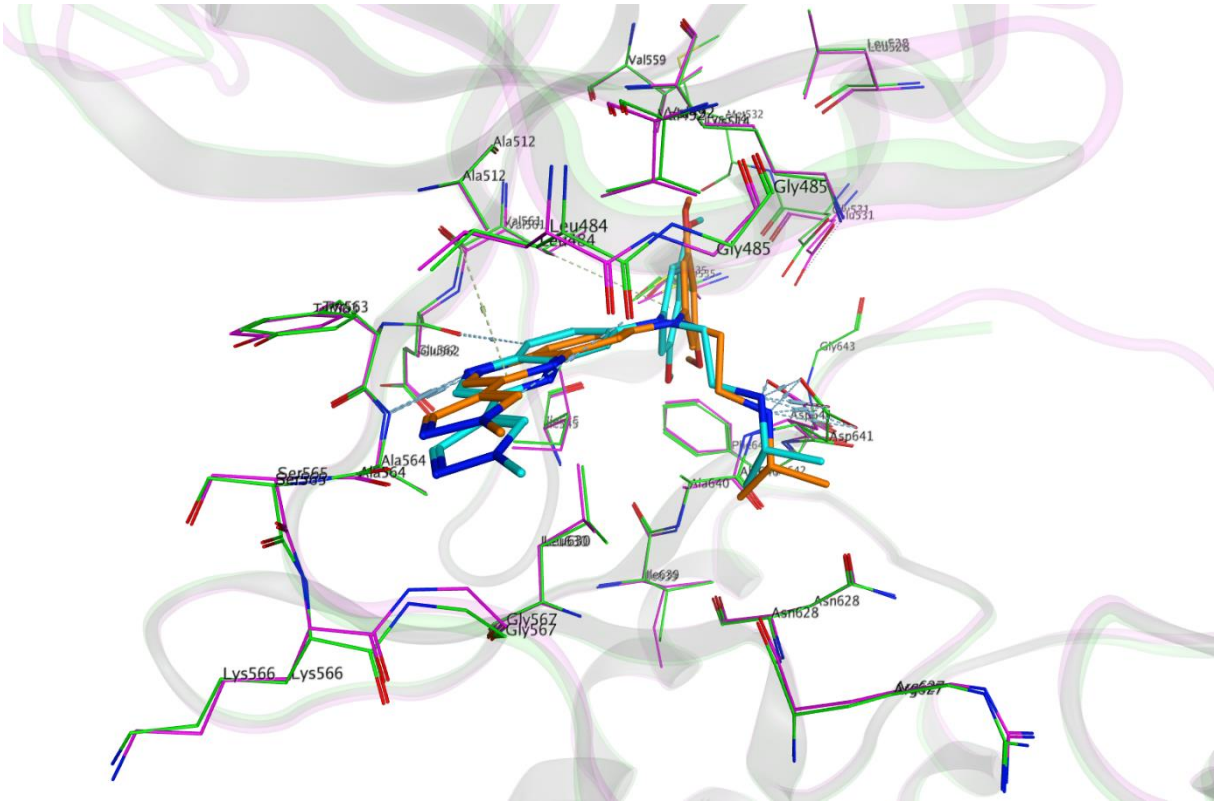

Figure S10. Superimposition of the crystal structure of erdafitinib-FGFR1 complex (Pdb id: 5ew8.pdb) with the best ranked docking pose of erdafitinib inside the prepared structure of FGFR1 from 3rhx.pdb. Cyan and orange sticks represent erdafitinib in the crystal structure and the prepared structure of FGFR1, respectively. The active site residues are named using three letters code and represented as magenta sticks in the crystal structure of FGFR1 (Pdb id: 5ew8.pdb) and as green sticks in the prepared structure of FGFR1. The backbone structure of the crystal structure of FGFR1 (Pdb id: 5ew8.pdb) and the prepared structure of FGFR1 are represented as magenta and green ribbons, respectively. H bonds and CH–π interactions are represented by pale blue and pale green dashed lines, respectively. For clarity, all hydrogen atoms have been removed.

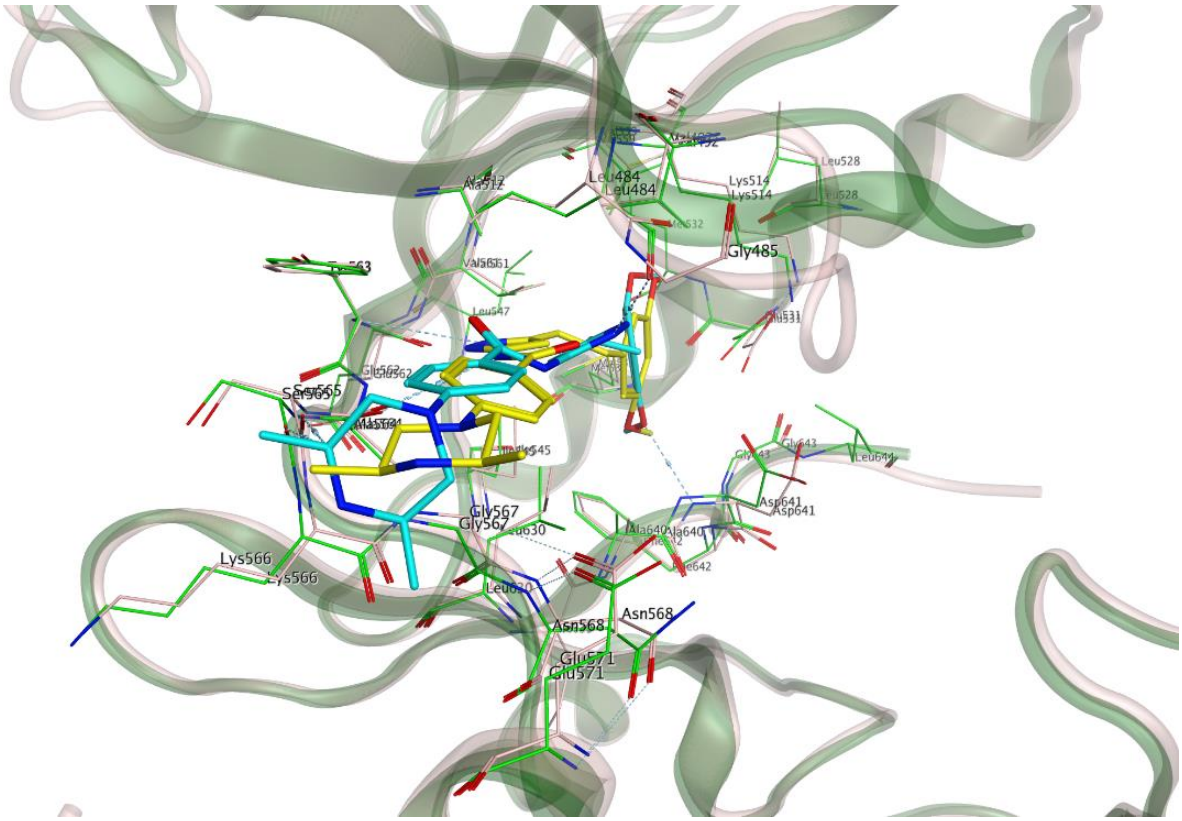

Figure S11. Superimposition of the crystal structure of AZD4547-FGFR1 complex (Pdb id: 4v05.pdb) with the best ranked docking pose of AZD4547 inside the prepared structure of FGFR1 from 3rhx.pdb. Yellow and cyan sticks represent AZD4547 in the crystal structure and the prepared structure of FGFR1, respectively. The active site residues are named using three letters code and represented as pink sticks in the crystal structure of FGFR1 (Pdb id: 4v05.pdb) and as green sticks in the prepared structure of FGFR1. The backbone structure of the crystal structure of FGFR1 (Pdb id: 4v05.pdb) and the prepared structure of FGFR1 are represented as pink and green ribbons, respectively. H bonds and CH–π interactions are represented by pale blue and pale green dashed lines, respectively. For clarity, all hydrogen atoms have been removed.

Table S4. Docking scores and first ranking poses for FGFR inhibitors inside FGFR1 (Pdb id: 3rhx), using Goldscore.

Compounds	GoldScore	3D Interaction of first ranking poses of hit
Erdafinitinib	85.75 (1)	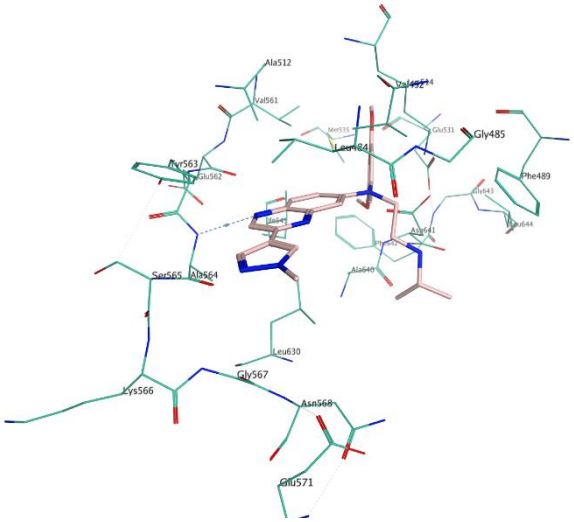
Lenvatinib	66.11 (1)	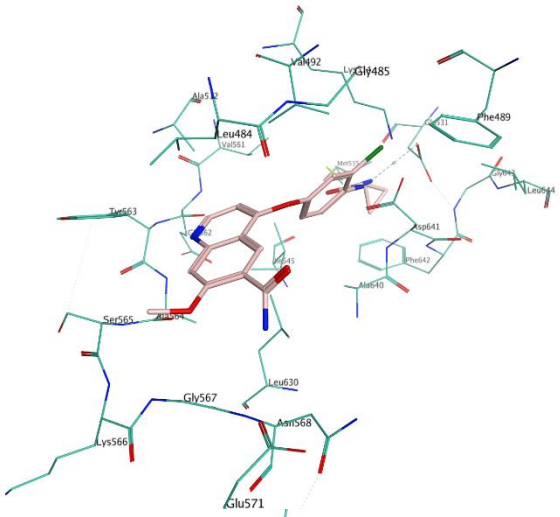
Dovitinib	63.97 (1)	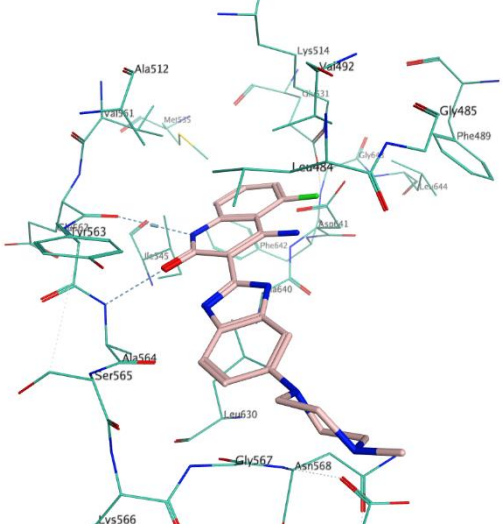

AZD4547	71.21 (1)	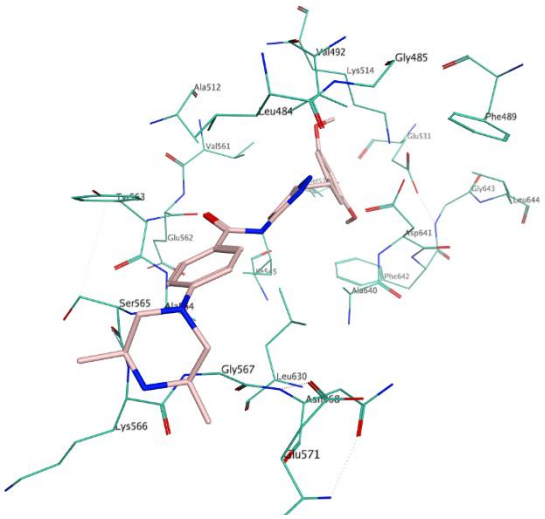

Table S5. MM-GBSA free binding energies (DELTA TOTAL) of the inhibitors in FGFR1.

Compound	**Erdafinitinib**	**AZD4547**
VDWAALS (kcal/mol)	-58.1595 ± 0.3354	-53.7440 ± 0.3101
EEL (kcal/mol)	-104.4298 ± 1.3031	4.2426 ± 1.0395
EGB (kcal/mol)	113.5529 ± 1.1392	9.1269 ± 1.0505
ESURF (kcal/mol)	-7.4845 ± 0.0283	-6.4363 ± 0.0263
DELTA G gas (kcal/mol)	-162.5893 ± 1.2278	-49.5015 ± 1.1403
DELTA G solv (kcal/mol)	106.0684 ± 1.1370	2.6906 ± 1.0476
DELTA TOTAL (kcal/mol)	-56.5209 ± 0.3255	-46.8109 ± 0.4002

Table S6. Calculated molecular descriptors for compound **G1-G22** using MOE 2016

Compounds	logP(o/w)	H Bond Acceptor	H Bond Donor	Molecular Weight
G1 (ID:316803)	0.4481	4	3	547.449
G2 (ID:102217)	1.571	3	1	551.219
G3 (ID:1572237)	4.724	5	1	450.543
G4 (ID:1253838)	5.0108	4	2	505.884
G5 (ID:1084268)	-0.0559	4	2	490.397
G6 (ID:335949)	3.239	6	2	553.643
G7 (ID:230615)	5.6755	6	1	482.632
G8 (ID:219085)	3.545	5	2	554.478
G9 (ID:1088295)	6.3828	4	1	529.566
G10 (ID:151959)	6.536	3	2	454.57
G11 (ID:218049)	4.3205	6	2	488.616
G12 (ID:461758)	3.711	5	1	514.614
G13 (ID:150405)	6.902	2	2	456.61
G14 (ID:367127)	4.724	9	7	569.552
G15 (ID:518166)	3.9551	5	1	510.538
G16 (ID:593813)	4.7201	7	6	529.004
G17 (ID:605410)	3.3441	8	6	519.5690
G18 (ID:514509)	6.528	4	2	508.581
G19 (ID:358843)	4.915	3	2	472.609
G20 (ID:392998)	4.0655	4	1	551.611
G21 (ID:359316)	5.922	3	2	440.543
G22 (ID:1596766)	3.882	5	2	434.52

Table S7. ATP binding site residues of FGFR1 (Pdb id:3rhx)

ATP binding site residues
LEU484, GLY485, PHE489, VAL492, ALA512, VAL513, LYS514, GLU531, MET535, ILE545, VAL559, ILE560, VAL561, GLU562, TYR563, ALA564, SER565, LYS566, GLY567, ASN568, LEU569, ARG570, GLU571, ARG627, ASN628, VAL629, LEU630, ILE639, ALA640, ASP641, PHE642, GLY643, LEU644